Smartwatch-Embedded Biosensors For Healthcare Monitoring

Vivien PERRELLE

Research in biological sensors for healthcare applications has grown exponentially, driven by the recent advances in IoT and microtechnology. However, a noticeable gap remains in the availability of commercialized wearable systems for painless, unobtrusive biomonitoring experiences. This master's thesis presents the iterative development of a smartwatch prototype - the *BioWatch* - for implementing non-invasive and discreet wearable biosensors. The BioWatch's connectivity allows biosensor module integration and wireless connection to stand-alone sensor systems. A sweat glucose biosensor and a microneedle lactate biosensor are developed for the BioWatch. Three continuous glucose monitoring (CGM) users tested the BioWatch. All would rather wear a smartwatch-like CGM similar to the BioWatch than their current CGM. The results of this research work advocate a comprehensive design methodology, emphasizing technical performance, user experience, and medical relevance as the foundation for developing future discreet and pain-free biomonitoring systems. The proof-of-concept presented contributes to developing wearable platforms for non-invasive biomarker monitoring. Integrating biosensors into smartwatches can drastically improve the daily lives of chronically ill patients and the general population healthcare.

Contents

Introduction 1

1.1 Context

1.1.1 Wearable Health Technologies

The recent expandingly integration of wireless communication technologies in everyday objects is known as the *Internet of Things* paradigm (IoT) [1] IoT technologies have enabled the development of wearable devices to enhance daily life through seamless connectivity and automation [2].

Wearable devices, or *Wearables*, refer to hand-free smart and wireless electronic gadgets, accessories, or clothes worn on the human body, or even invasive versions such as microchips or smart tattoos [3, 4]. The field of wearable technology has witnessed significant advancements throughout history, with notable milestones marking the progression of innovative devices. In 1961, Edward O. Thorpe and Claude Shannon, researchers from MIT, pioneered the concept of wearable computing by concealing a timing device in a shoe [5]. Since then, wearable technologies have grown exponentially [6]. Hundreds of commercialized products enable new applications, address new user needs, and create new markets [7]. Massive investment from the public and private sectors has enabled disruptive innovations and the democratization of wearables [8].

Figure 1.1: Most researched wearable IoT application clusters. From [9]

Main wearable devices

Primary wearable devices include smartwatches, fitness trackers, smart glasses, and smart clothing [9]. Smartwatches are IoT devices that combine traditional watch functionality with a micro-computer capability [10]. They are equipped with microcontrollers, sensors, and application software that allow users to perform several tasks and track data [11]. Fitness trackers, or activity trackers, are wrist-worn devices that monitor

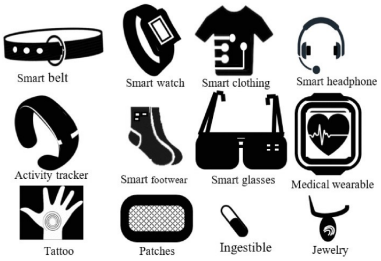

Figure 1.2: Different wearables developed for various applications. From [9]

various aspects of a person's physical activity and health. They are designed to help individuals keep track of their fitness goals, monitor their progress, and make informed decisions about their health and well-being [12]. Smart glasses feature a transparent screen on their electronic lenses to give users a hands-free computing experience. They typically include a camera, microphone, and speaker, and are controlled through voice commands, touch, or gestures [13]. Finally, smart clothing, or e-textiles, refers to wearable artifacts composed of textiles that incorporate electronic, computational, and sensory functionalities to convert environmental stimuli into aesthetic or physical responses [14].

General use of wearables

Wearable devices have become increasingly popular in recent years due to their versatility. These devices cover various applications, including health and fitness monitoring, communication, and entertainment. Wearables track vital - like pulse, respiratory rate, body temperature - and non-vital signs - such as blood pressure and blood oxygen - providing valuable information for the wearer [9, 16]. They monitor physical activity, calorie expenditure, sleep patterns, nutrition and stress levels helping users to improve their overall health and well-being [17]. Wearables, mainly smartwatches, are also used for communication, such as receiving notifications, making calls, and sending messages. Some non-permanently worn devices, including smart glasses, headphones and headsets, provide entertainment through video streaming, music, gaming, and virtual reality [18]. The main functional innovation of wearables is their ability to provide users with quick and easy access to information and services without pulling out a phone or other portable device [19].

Wearable technology for healthcare applications

Wearable technologies have disrupted traditional paradigms in healthcare by offering a holistic approach to health monitoring and management. Unlike conventional smartphones and tablets, these devices are adept at capturing

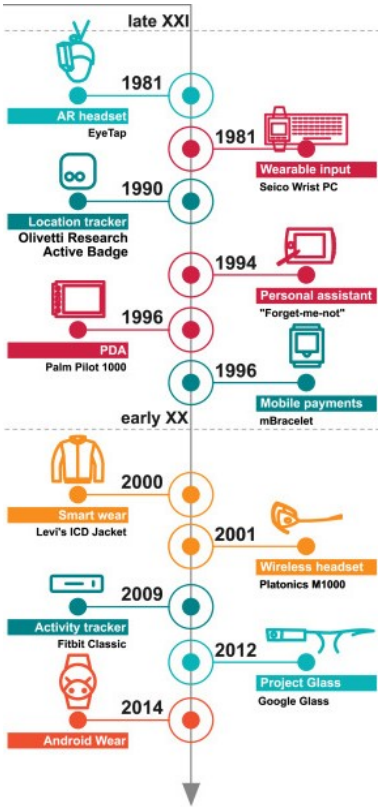

Figure 1.3: Main innovations in wearable technologies since 1980.. From [15]

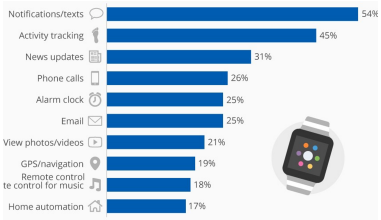

Figure 1.4: Owner's daily use of smartwatch functions. Based on a survey of 5,000+ U.S. consumers, aged 18+ from diverse regions and demographical backgrounds. From [20]

rich contextual information directly from our bodies [4]. With the ability to track individual health metrics and offer tailored diet, exercise, and lifestyle modification recommendations, wearables provide personalized healthcare solutions [22]. These devices facilitate the real-time transmission of health data to healthcare providers, enabling remote patient monitoring [23, 24]. Embedded machine learning algorithms further enhance their utility by identifying unusual patterns in health data and issuing timely health event predictions and warnings [25]. Finally, wearables are motivational tools, empowering patients to actively engage in their healthcare journey [26, 27]. Beyond enhancing user experience, wearables have unlocked a plethora of functionalities, holding great potential for improving healthcare outcomes.

Figure 1.5: Main health and activity indicators monitored with wearales. From [21]

Challenges and Limitations in Health Data Relevance

Despite the remarkable progress in developing and adopting wearables in the well-being, fitness, and lifestyle sectors, their integration into the healthcare environment remains a complex challenge [28]. Many commercially available wearables have inherent limitations in the scope of health data [29]. They often measure only a handful of health-related indicators with limited diagnostic relevance [30, 31]. Critical health markers such as heart rate variability, nutrition, and mood, crucial for comprehensive health assessment, continue to elude accurate measurement through wearables [17, 32, 33]. Moreover, despite substantial investments and efforts toward harnessing wearable data for patient care, only 10% of US physicians report integrating data from patient wearables into their electronic health records [29]. This limited adoption can be attributed to both technical constraints and regulatory challenges. Wearables cannot diagnose or treat medical conditions independently nor provide actionable insights to healthcare professionals [31].

A rigorous and systematic research effort is essential to develop a new generation of high-performance onboard sensors for wearables. **Wearable technology must undergo a thorough investigation to gain accuracy,**

completeness, and impact on clinical workflows and seamlessly integrate clinical practice [22]. Recent advances in microtechnology, particularly in biosensing, offer exciting prospects for acquiring highly relevant medical data, enriching the capabilities of wearable devices [34].

1.1.2 Wearable Biosensors for Healthcare

Wearable sensors are key components of wearable devices [36]. They are classified into motion state, biophysical and biochemical sensors [37]. Biochemical sensing is particularly promising for measuring relevant contextual medical data. *Biosensors* – for *biochemical sensors* or *biological sensors* – are probes that integrate a biomolecule recognition system with an electronic transducer [38, 39]. By measuring a specific biomolecule concentration, biosensors convert a biological response into an electrical signal, with high sensitivity, specificity, and speed [40]. The potential of biosensing in wearable technologies lies in its ability to provide real-time, continuous, and non-invasive health analysis at the molecular level [41]. Integrating biomolecule detection functionalities with wearable devices allows the monitoring of accessible biomarkers from the human body. Collecting large-scale biochemical information about an individual's dynamic health status empowers personalized and precise healthcare interventions [42].

Biosensing technologies

Due to their ability to detect and monitor specific biological responses, biosensors have been widely used and developed for laboratory applications since 1960s, for in vitro detection [44]. The concept of biosensors for measuring biomarker levels was first proposed in 1962 by Clark and Lyons from the Children's Hospital of Cincinnati [45]. In 1967 Updike et al. developed the first biosensors [46]. The miniaturized system presented continuously measures glucose levels thanks to an immobilized enzyme. The first microbial biosensor was made in 1975, the first bedside artificial pancreas in 1976

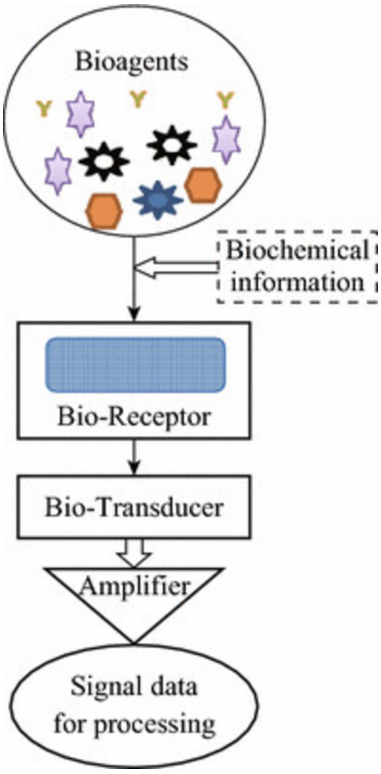

Figure 1.6: Basic principles of a biosensor. From [35]

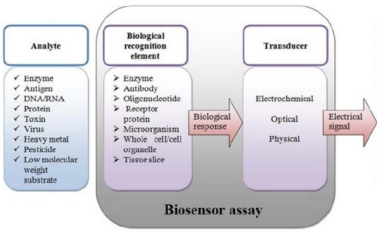

Figure 1.7: Principle of biosensor operation and main components: the analyte is detected by the biologically-affined sensitive layer, immobilized on the transducer. The biological response is transformed to an electrical, optical or electrochemical signal by the transducer and then further processed, providing the information. From [43]

[47], and the first plasmon resonance immunosensor in 1984, among other essential biosensing mechanisms [48]. Recent research has led to the mastery of new technologies for biodetection. Biosensors became highly diverse, and classified according to several conceptual characteristics. The main ones are:

1. the target element: metabolites (glucose, lactate, alcohol...), electrolytes (sodium, potassium, magnesium...), proteins, nucleic acids, amino acids, fatty acids, peptides, lipids, hormones, metals, pathogens, drugs... ;
2. the recognition element involved: enzyme, aptamer, antigen, peptides, CRISPR... ;
3. the recognition signal: electrochemical impedance spectroscopy (EIS), chronoamperometry (CA), cyclic voltammetry (CV), heat, mass change... ;
4. the transduction principle: electrochemical, optical, piezoelectric, thermal, magnetic, electrochemiluminescence... ;
5. the substrate material: natural materials (cotton, silk, wool...), inorganic materials (copper, gold, silver, platinum, graphene, carbon nanotubes...), synthetic polymers (silicone, polyvinyl alcohol, polyimide...) and hydrogels (alginate, agarose, polyethylene glycol...) [36, 49].

Emergence of wearable biosensors

With the growing development of wearable technologies, new biosensor applications have emerged outside laboratories. Medical technologies, including biosensor technologies, became wearable in the 2000s [52]. This paradigm shift marked the convergence of cutting-edge diagnostics and patient-centered care. Wearable biosensors operate in different biofluids: blood, sweat, interstitial fluid (ISF), urine, saliva, tears and exhaled breath [34, 49, 53, 54]. System electronics ensure autonomous measurement and processing. Connectivity features enable data communication to other portable or wearable devices. This transposition of the laboratory into contact with the body has become a promising way of improving patients' care, especially for the aged and

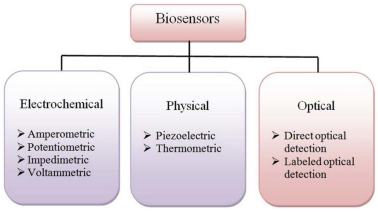

Figure 1.8: Types of biosensors based on their transducer operation. From [43]

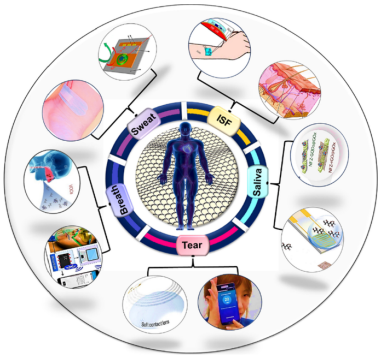

Figure 1.9: Illustration of main non-blood body fluids for biosensing applications. From [50]

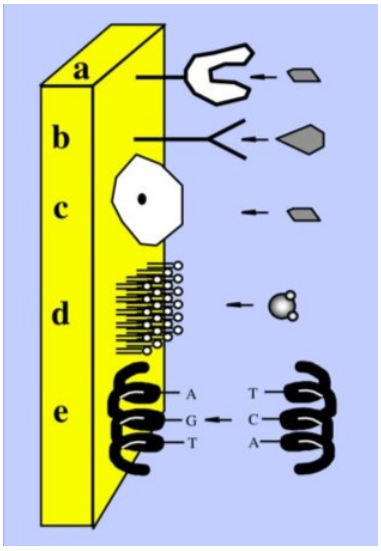

Figure 1.10: Cartoon of different types of electrochemical biosensors with different recognition element/target analyte: (a) enzyme/substrate, (b) antibody/antigen, (c) cell/substrate, (d) lipid monolayer/analyte, (e) single-stranded DNA/-complementary strand. From [51]

chronically ill, like people with diabetes [48, 55].

Potential of wearable biosensors in a technological world

Recent IoT innovations enable the collection, storage, transmission, processing, and analysis of a vast amount of health data generated from wearable devices [53]. This data can enhance medical research and clinical practices, improving individual health outcomes [58, 59]. **IoT-assisted wearable biosensors have the potential to revolutionize personalized medicine, chronic illness management, early disease detection, and preventive healthcare by providing valuable insights into an individual's molecular profile [41, 60].**

Figure 1.11: Picture of a glucometer. The first portable blood glucose meter was introduced by Anton Hubert Clemens in 1971 [56].

Figure 1.12: Picture of the first Continuous Glucose Monitoring (CGM) commercialized in 1999 by MiniMed [57]. The sensor is a needle inserted under the skin to measure glucose in the ISF.

Figure 1.13: Picture of the GlucoWatch G2 Biographer, the first wearable CGM.

1.2 Related Works

Commercial wearable CGMs

CGMs are medical devices primarily designed for individuals with diabetes to continuously monitor their blood sugar levels [61]. Their glucose biosensor allows users to continuously measure their glucose levels without requiring frequent finger pricks. CGMs were the first wearable systems to incorporate biosensors, partly due to the stability of the glucose enzyme and market demand.

Glucowatch was the first CGM marketed and approved by the FDA in 2001. The GlucoWatch Biographer is a non-invasive on-wrist CGM developed by Cygnus, Inc. that provides automatic, frequent, and non-invasive blood glucose measurements for type 1 diabetes, with a 12-hours autonomy [62]. The device performs reverse iontophoresis[1] to extract subdermal ISF through the skin. The electrochemical biosensor involves the enzyme Glucose Oxidase (GOx). GOx catalyzes the oxidation of glucose in the ISF to hydrogen peroxide, which is, in turn, oxidized. The electrical signal generated is measured by chronoamperometry. An alarm system warns the patient if hypoglycemia is detected, with a lag-time of 17.5 minutes on blood concentrations [64]. The GlucoWatch

1: *Iontophoresis* consists in applying a small electric current to enhance the migration of polarized and neutral ISF compounds through the skin [63].

Biographer detected up to 75% hypoglycemic episodes with a low false alert level 1. The GlucoWatch device was discontinued in 2007 due to the skin-burning effects causing users dissatisfaction.

Other invasive CGMs have appeared on the market since GlucoWatch. The best-known are the Freestyle Libre 3 from Abbott [67], the G6 CGM System from Dexcom [68] and the Guardian Sensor 3 from Medtronic [69]. These devices feature a needle inserted under the skin to measure glucose concentrations in the ISF. Despite great accuracy [70], these devices also present a poor user experience, as discussed in section 2.1.

Non-invasive and minimally-invasive wearable biosensors

Numerous scientific studies have attempted to **reconcile effective analyte monitoring with strong user experience**. Two new categories of biosensors have emerged: **non-invasive biosensors and minimally-invasive biosensors**. These aim to detect biomarkers without intruding beneath the skin.

Kim et al. (2018) developed a wearable biosensor platform that monitors sweat and ISF simultaneously [65]. The device detects glucohol (glucose + alcohol) levels in real-time. Monitoring this pair of analytes is particularly useful for insulin-dependent diabetics. The system consists of a wearable iontophoretic biosensor on a printed tattoo platform for glucohol sensing on a human subject. The biosensor is coupled with a wireless flexible printed circuit board. The biosensor operates through iontophoresis. The glucohol biosensor has a "panda-like" electrode layout with iontophoretic gels and layered composition of the working electrodes. The device uses amperometric detection thanks to alcohol oxidase (AOx) and GOx. Concentration data are wirelessly transmitted to a mobile app in real-time. Both biosensors showed excellent correlation with blood concentrations. The device developed by Kim et al. is pain-free, provides real-time and simultaneous monitoring, uses wireless transmission, and is easy to use. However, the biosensor remains visible, signaling a medical condition.

Figure 1.14: Picture of the Freestyle Libre 3 from Abbott Laboratories. The CGM is worn on the back of the arm.

Figure 1.15: Photo of the Dexcom G6 and its flexible needle.

Figure 1.16: Depiction of the wearable iontophoretic biosensor device developed by Kim et al. for glucose and alcohol monitoring on a human subject. A wearable app allows the user to read its glucohol levels. From [65]

Discreet, smartwatch-like biosensing systems

Several research teams have developed **wristband-integrated noninvasive biosensors with a display**, similar to a smartwatch. This design enables a better user experience with biosensors.

Zhao et al. (2019) developed a fully integrated and self-powered smartwatch for continuous sweat glucose monitoring [66]. The device includes flexible electrochemical sensors for non-invasive glucose monitoring. The enzyme-based biosensor generates an output amperometric signal, amplified by a transimpedance amplifier (TIA), and converted into a digital signal. The digital signal is analyzed, filtered out high-frequency noise, and processed to an electronic ink (E-ink) display. The E-ink module provides the merits of a stable display without a continuous power supply, ultralow power consumption, wide viewing angle, and high visibility and contrast. The integrated PCB and E-ink screen enable real-time and *in situ* data analysis/display, eliminating transmission units and external reading devices. The glucose levels are indicated on the smartwatch display as alarm signals from "low", "medium", to "high" The current detection resolution of the smartwatch based on the customized circuit can reach 6 nA, corresponding to a glucose concentration of around 2 μM. The wristband is a rechargeable and flexible Zn-MnO2 battery, powering the smartwatch with energy harvested and converted by photovoltaic cells. The system accuracy was tested with sweat samples collected from subjects during ergometer-based cycling exercises. The smartwatch developed by Zhao et al. is a user-friendly device that provides non-invasive and continuous monitoring of sweat glucose levels, real-time display, and self-powered functionality.

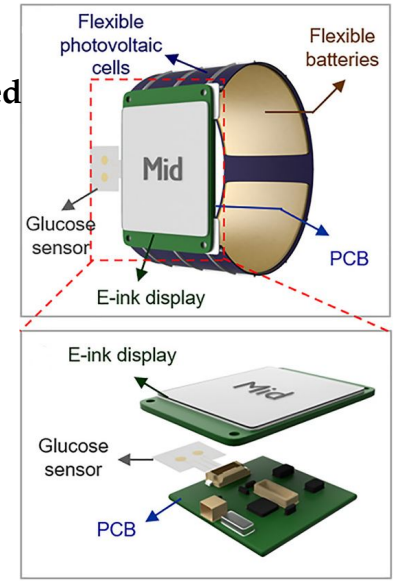

Figure 1.17: Schematic illustration of the self-powered CGM smartwatch developed by Zhao et al. From [66]

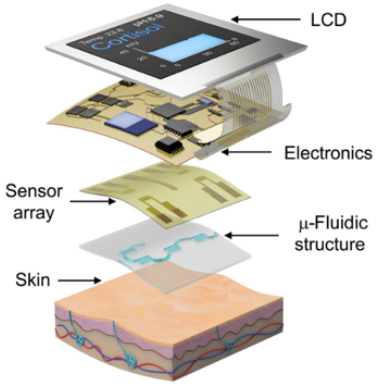

Figure 1.18: Expanded view of Wang et al. wearable system, where the sensor array, microfluidic module, flexible PCB, and LCD components form a multichannel biosensing smartwatch. From [71]

Wang et al. (2022) developed an aptamer-field-effect transistor (FET) biosensing device for monitoring cortisol levels in human sweat [71]. The device is integrated into a smartwatch and a smartphone application, allowing wireless and label-free detection. The aptamer-FET biosensor is a non-invasive and convenient method for

monitoring cortisol levels, a stress biomarker. Biosensor aptamers bind to the target molecule, causing a change in the electrical properties of the FET. The device was tested on 88 human subjects, and the detection limit was 0.001 nM. The device measures cortisol levels in real-time with high precision and sensitivity, making it a promising tool for stress management and healthcare applications. The sensor non-invasiveness, real-time monitoring, and smartwatch integration demonstrate excellent user experience.

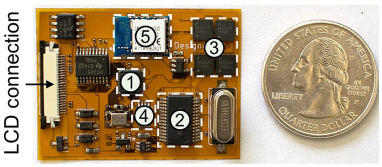

Figure 1.19: Photograph of the Wang et al. flexible PCB next to a U.S. quarter. The components are (1) MCU, (2) ADC, (3) potentiostat chip, (4) digital-to-analog converter, and (5) Bluetooth. From [71]

Chang et al. (2022) developed a highly integrated watch for noninvasive continual blood glucose monitoring [72]. The watch employs a Nafion-coated flexible electrochemical sensor patch fixed on the watchband. Reverse iontophoresis extracts ISF transdermally at the wearer's wrist. The watch's LED screen and a smartphone application display real-time blood glucose levels. The watch demonstrated 84.34% clinical accuracy in the Clarke error grid analysis with 23 volunteers. The watch-like design ensures comfortable daily wear, facilitating continual glucose monitoring.

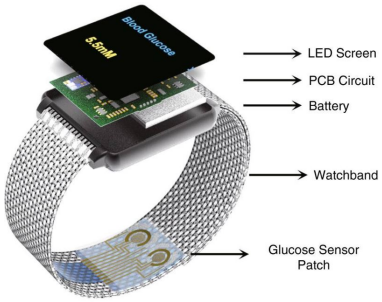

Figure 1.20: Exploded view of the watch developed by Chang et al. for noninvasive continual glucose monitoring. From [72]

Finally, bio-wearable company PKvitality is the first to develop a commercial smartwatch incorporating minimally-invasive biosensors [74]. The K'Watch is a smartwatch incorporating a disposable module of painless micro-needles - the K'apsul [73]. Depending on the sensor functionalized on the needles, the K'watch monitors glucose levels in the ISF for diabetics (K'Watch Glucose [73]) or lactate levels for athletes (K'Watch Athletes [75]). A hypoallergenic adhesive patch holds the K'apsul in place. A smartwatch vibration alerts the user in case of a hypo- or hyperglycemic crisis. The biosensor is easily replaceable after its seven-day lifespan. Begun in 2018, the K'Watch development is still in progress. PKvitality's technology would ensure an optimal health experience with biosensors by being painless and seamlessly integrated into a fashionable electronic object.

Figure 1.21: Illustration of the Kapsul: the replaceable microneedles biosensor module for the K'Watch. From [73]

1.3 Problem Statement

Wearable molecular detection systems currently on the market offer a poor user experience. CGMs are invasive, painful, and cost-expensive [76]. They signal an invisible disease, are considered unattractive by patients, and lead to information overload [77]. Additionally, using a cell phone to check glucose levels is necessary, and may be unsuitable in certain situations. Single biomarker biosensors commercialized also lead to limited health data relevance [78]. Implementing non-invasive biosensors in smartwatches would overcome these limitations.

Figure 1.22: Illustration of the K'Watch. From [74]

1.4 Scientific Contribution of the Thesis

The first contribution lies in developing a smartwatch platform to integrate biosensors for prototyping and proof-of-concept purposes. The device allows rapid implementation and on-body tests of non-invasive (sweat) or minimally-invasive biosensors (ISF). A user study enabled the design of a user experience adapted to glucose monitoring for people with diabetes. Design study also contributes to a better understanding of the user experience for wearers of smartwatches with integrated biosensors.

The second contribution is developing and integrating a micro-needle-based enzymatic lactate sensor for the BioWatch. The fabrication of the microneedles, the functionalization, and in vitro testing are covered. Additionally, a review of scientific literature on lactate pharmacology contributes to understanding lactic acid evolution and ISF monitoring during physical effort. An interactive web application accompanies this research. The app, named Bione, is the first interactive educational application to teach the principles of biosensors.

The following work presents a transdisciplinary approach between applied science: biotechnology, electronics and programming; exploratory research: phys-

iology; and user experience science. Beyond technical contributions, this thesis proposes an innovative vision of a central wearable platform for real-time visualization of advanced health data from different wearable biosensors.

The following research represents a significant stride towards realizing the vision of comprehensive and user-friendly health monitoring through wearable technology.

1.5 Structure of the Thesis

The thesis is divided into two main sections. In the initial section (Chapter 2), we delve into the development of the BioWatch, encompassing both technical advancements and user experience research. the assembly of a glucose sensor and its wireless connection to the BioWatch is covered. The second section (Chapter 3) is dedicated to the creation of a microneedle-based lactate biosensor. We detail the technical work and comprehensively review lactate pharmacology for minimally-invasive measurements. Additionally, we explore the development of an educational biosensor web application.

In carrying out this work, we have considered the reproducibility of the results. The work described is open-source and published on GitHub [79]. Tutorials and project presentations are available on vivienperrelle.com and the DVIC website [80] to ensure the transferability of the knowledge acquired.

The BioWatch: A Smartwatch for Wearable Biosensors

2

2.1 Introduction

Smartwatches were the first socially accepted wearable devices. The smartwatch's popularity is attributable to the interplay between a fashion accessory and a disruptive technological gadget [81]. The wearables market has experienced significant growth since 2014, driven by the increasing popularity and adoption of smartwatches. Some leading wearable device manufacturers include Apple, Samsung, Fitbit, Garmin, and Xiaomi. Their high and steady product innovation responds to market needs, with more than 230 million wearables shipped in 2021 and a constant annual growth of 20% [4]. Smartwatches are the most sold wearable, with around 130 million units sold [82, 83]. Most technologically advanced smartwatches perform various functions, including tracking activity, monitoring health, and smartphone connectivity [84]. Various miniaturized sensors collect data and provide feedback to the user to perform these functions. Some standard sensors integrated into smartwatches include accelerometers, heart rate monitors, gyroscopes, GPS, and ambient light sensors.

1. Accelerometer: To measure the watch's acceleration and track the wearer's movement and activity level.
2. Gyroscope: To measure the orientation and rotation of the watch to track the wearer's movements and gestures.
3. Heart rate monitor: This sensor uses photoplethysmography (PPG) to measure the wearer's heart rate by detecting changes in blood volume in the wrist.
4. GPS: Built-in GPS sensors allow to track the wearer's location and provide navigation assistance.
5. Ambient light sensor: To adjust the brightness of the watch's display based on the surrounding light

Figure 2.1: Commercial illustration of the Apple Watch series 9 with its sleep monitoring interface. From [85]

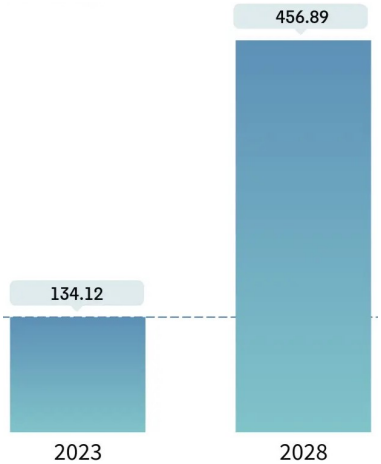

Figure 2.2: Smartwatch shipment volume in million units estimated by Mordor Intelligence. Compound Annual Growth Rate is around 27.8% between 2023 and 2028. From [86]

conditions.

6. Barometer: To measure changes in air pressure to predict weather changes and track altitude during activities like hiking.
7. Microphone: A built-in microphone allows the wearer to make phone calls, send messages, and use voice commands to control the watch.

Figure 2.3: Exploded view of the Apple Watch. From [87]

The sensors integrated into smartwatches vary depending on the manufacturer and the device's intended use. Smartwatches have evolved from simple timekeeping devices to multifunctional wearable devices that track various health and fitness aspects. Although smartwatches are the best-selling wearable, they do not integrate biological sensors. Their sensors remain limited to biophysical ones [88].

Commercialized CGMs limitations

The only wearables on the market incorporating biosensors are continuous glucose monitoring (CGM) wearables. These devices result in narrowed user experiences. On the arm or stomach, CGMs are 2 to 5 centimeters in diameter, visible when wearing a t-shirt or bathing suit. Diabetic patients feel stigmatized by body signs of diabetes [89, 90]. Moreover, the sensor installation is painful. Current CGMs are invasive, measuring glucose concentration in the subcutaneous interstitial fluid [91]. They feature a flexible, functionalized needle, penetrating a few millimeters beneath the skin. Placement is, therefore, unpleasant, particularly for children and people prone to fear of needle-related procedures [92]. Commercially available diabetes monitors also present high premature loss frequency. Adhesive can cause skin irritation and hypersensitivity [93]. Lastly, CGMs are relatively expensive and not environmentally friendly either. The biosensor lifespan varies from 7 to 14 days, for a few tens of dollars per unit price. The entire device is thrown away, even though the electronics are not obsolete [94]. Using smartwatches for non-invasive or minimally-invasive biosensors is a promising solution to these user experience and recycling issues.

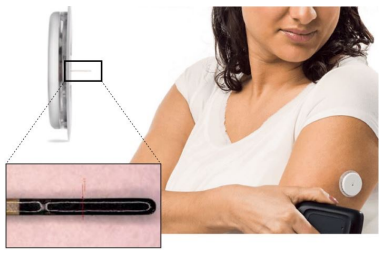

Figure 2.4: Abbott FreeStyle Libre Flash Glucose Monitoring System. The insertion sharp is a slotted needle with a cross-sectional area of 0.29 mm^2 and a length of 8.5 mm. From [95]

Smartwatch: the future platform for wearable biosensors

Technical advances enable the detection of a wide range of molecular biomarkers. **The scientific advances in wearable biosensors could match the growing success of smartwatches.** Indeed, users perceive smartwatches as functional sensors rather than watches or smartphones [96]. The community eagerly awaits new sensing functions, as smartwatches grow increasingly powerful. **Implementing molecular detection is one of the next landmarks for smartwatch development.** Other embedded technologies, such as artificial intelligence, could duplicate the biosensing potential for healthcare [97–99]. Already smartwatch-embedded physical sensors also bring synergy to biosensors. The potential to provide a more comprehensive and accurate depiction of an individual's health status by combining biophysical and biochemical data.

Figure 2.5: The wearable freestanding electrochemical sensing system similar to a smartwatch developed by Zhao et al. [100]. Credit: Yichao Zhao/UCLA [101]

This section presents the development of the BioWatch. **The BioWatch is an electronic prototyping platform aiming to easily demonstrate proof of concept of non-invasive electrochemical biosensors integrated into a smartwatch or wirelessly connected**. Three smartwatch versions are released, following a structured development process to meet the final product's functionality and performance targets. We granted emphasis on the user experience. The vision of this project is not only to design a technical proof-of-concept for a biosensor smartwatch but also to demonstrate acceptance by potential users. The BioWatch is the first turnkey prototyping solution for developing smartwatches with smartwatches-integrated biosensors. Although further research is needed to achieve this ideal, this open-source work provides a methodological basis for the academic community and future guidelines. **The BioWatch aims to bridge the gap between cutting-edge biosensing technology and wearable smartwatches.**

2.2 Hardware Development

2.2.1 BioWatch V1: Proof-of-Concept

The first development milestone is to create a non-wearable prototype of a smartwatch. This prototype serves as the foundation for the subsequent iterations of the device. We first selected an appropriate display, balancing cost-effectiveness with the capability to present essential numeric information. After a thorough evaluation, we opted for a GC9A01 round LCD module, RGB and backlit screen from WaveShare, acquired for 14 euros.

Figure 2.6: Waveshare round LCD module display. From [102]

The display boasted a resolution of 240x240 pixels for a 3.25-centimeter diameter, meeting our requirements for showcasing data effectively.

An electronic board Arduino Uno R4 pilotes the GC9A01 module. This choice was driven by its wide adoption and compatibility with the display driver. The display operated on a 3.3V input signal and utilized I2C communication for data transfer. A clock example Arduino code is uploaded to print a classic watch face with hands on the screen. A computer or an external battery powers the board.

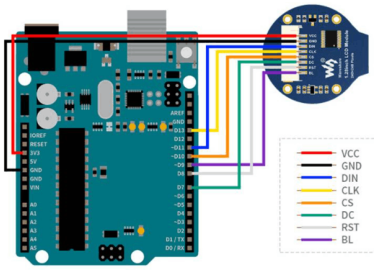

Figure 2.7: Wiring of Arduino Uno board with GC9A01 module.

Figure 2.8: Display after uploading a code from the manufacturer Waveshare.

The screen enclosure was meticulously crafted using CAD software and 3D printed in polylactic acid (PLA), ensuring a precise fit. The first version of the BioWatch only includes the CG9A01 module in the case. Precise measurements were translated into a technical schematic, and SolidWorks aided in designing the enclosure with considerations for microcontroller, passive components, and retaining screw locations. A side window allows the wires to reach the development board.

Figure 2.9: Back of module GC9A01, with the four screw slots visible.

(a)

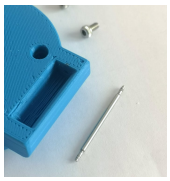

(b)

Figure 2.10: (a) Incremental development of the 3D case model. (b) A rod next to the insertion slot for attaching the watch strap.

Four 4mm-diameter screws on the screen's back were utilized initially to enhance stability. We secure the screen with the screws provided in the GC9A01 module. The screws fortify the system, preventing the screen from falling when the watch is face down. Watch strap attachment allows one to attach the watch to the wrist.

Figure 2.11: First version of the BioWatch.

2.2.2 BioWatch V2: Autonomy and portability

In this phase of BioWatch development, the primary objective was transforming the conceptual framework into a wearable and autonomous apparatus. This was achieved by incorporating a Lithium-Polymer (Li-Po) battery and a corresponding battery shield.

Facilitating the transition of the BioWatch into a wearable device necessitated the replacement of the initial Arduino Uno microcontroller with the ESP8266 WeMos D1 Mini Lite microcontroller. The selection of the WeMos D1 Mini is predicated on its suitability for wearable applications, attributed to its compact dimensions measuring 34 x 25 mm. Notably, the ESP8266 microcontroller's Wi-Fi capabilities were aligned with the envisioned future functionalities of the device. Breadboard tests were conducted to ensure seamless compatibility between

the GC9A01 display module and the ESP8266 microcontroller.

A pivotal enhancement introduced in Version 2 entailed the integration of a battery shield onto the WeMos D1 Mini. This integral addition facilitated the power supply to the BioWatch through a 3.7V Li-Po battery, accomplished via a conveniently located mini JST connector. The incorporated Li-Po battery is a 30 x 20 millimeter LP502030 with a voltage rating of 3.3V and a capacity of 250mAh. Furthermore, the battery is conveniently recharged through the integrated micro-USB port within the shield. Two red and green LEDs offer essential battery status information to users and indicate the charging process and completion(figure 2.13). The interconnection of the two components was achieved by soldering male pins with minimal spacing. Subsequently, the GC9A01 display module was connected to the WeMos D1 Mini via wires of precise dimensions.

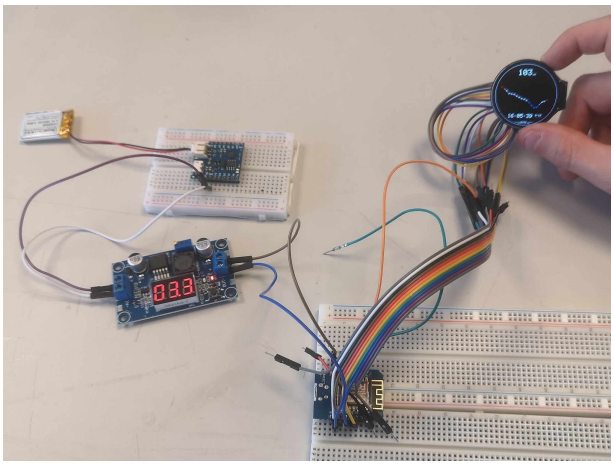

The design of the Version 2 screen enclosure drew upon the blueprint of the V1 iteration with meticulous attention to achieving a size optimization with a precision of 0.1 millimeters. The casing is fabricated using PLA material through a Prusa Mini printer configured for precision at 0.05 millimeters. A novel enclosure element, was introduced, replacing the conventional screw fastening mechanism for housing the electronic components. The cover, with a mere 2-millimeter thickness, aligns precisely with the surface of the display screen.

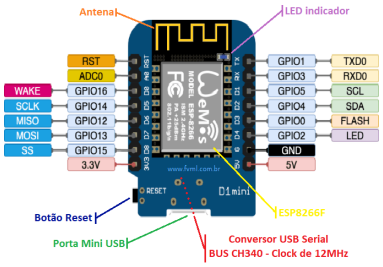

Figure 2.12: WeMos D1 mini is a miniature microcontroller development board.

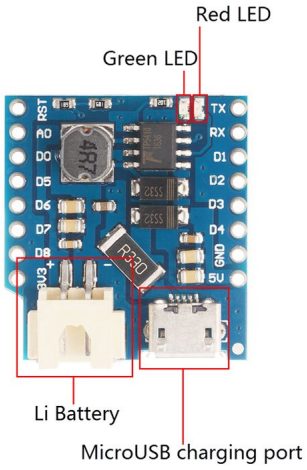

Figure 2.13: WeMos D1 mini battery shield.

Figure 2.14: BioWatch V2 hardware prototyping setup before miniaturization.

Version 2 represents a significant milestone in the evolution of the BioWatch, marking the transition from a static prototype to a wearable device characterized by enhanced autonomy. The successful integration of the Li-Po battery, battery shield, and the ESP8266 WeMos D1 Mini microcontroller has substantially advanced the prototype's resemblance to a fully functional smartwatch.

2.2.3 BioWatch V3: biosensors reception

The subsequent phase of development encompasses the transformation of the smartwatch into a biosensor platform, necessitating the integration of electronic circuitry for signal processing. Two distinct PCBs have been devised for this purpose: one exclusively dedicated to the smartwatch's operation, which combines the WeMos and the battery shield, and a second PCB housing the electronic components for modular biosensors.

The ESP8266 microcontroller originally present in the WeMos has been replaced with the ESP32 Wroom module, selected for its compact form factor and low power consumption characteristics. This choice is further justified by the ESP32's incorporation of Wi-Fi, Bluetooth, and Bluetooth Low Energy (BLE) modules, ensuring robust connectivity for the BioWatch. Additionally, the microchip is suited for wearable applications due to an extensive range of peripheral interfaces, encompassing SPI, I2C, UART, and ADC.

Figure 2.15: ESP32 Wroom dimensions.

Including a UART pinout has augmented the programmability and versatility of the ESP32. Seven digital pins have been allocated for programming the GC9A01 driver via the SPI interface, while the Li-Po battery connects to the circuit through designated pins. User convenience is enhanced by integrating a switch button, facilitating the on-off control of the smartwatch. Like the Wemos battery shield, a charging circuit allows for battery recharging via the micro-USB connector. Furthermore, two LEDs indicate the battery charge status and four female SPI pins enable connectivity to the second PCB dedicated to

biosensors.

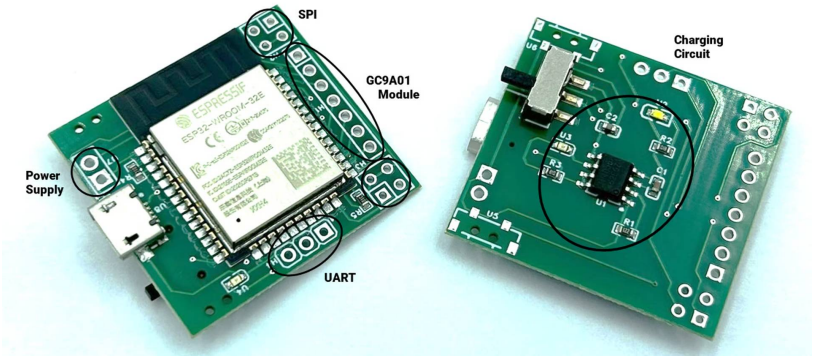

Figure 2.16: Custom-designed PCB for BioWatch version 3.

The design of the second PCB draws inspiration from the LMP91000 electronic board, a programmable analog front-end (AFE) suitable for micro-power electrochemical sensing applications. Extensive laboratory testing with an LMP91000 was conducted to develop the requisite Arduino code, and both PCBs can be closely stacked.

The watch case has undergone a redesign to accommodate the newly integrated PCBs. Small 2-millimeter-diameter magnets have been seamlessly incorporated into the 3D-printed watch case, facilitating the convenient attachment of sensors, including a micro-needle module beneath the BioWatch. Pin connectors establish the critical link between disposable non-invasive or minimally-invasive biosensors and the smartwatch.

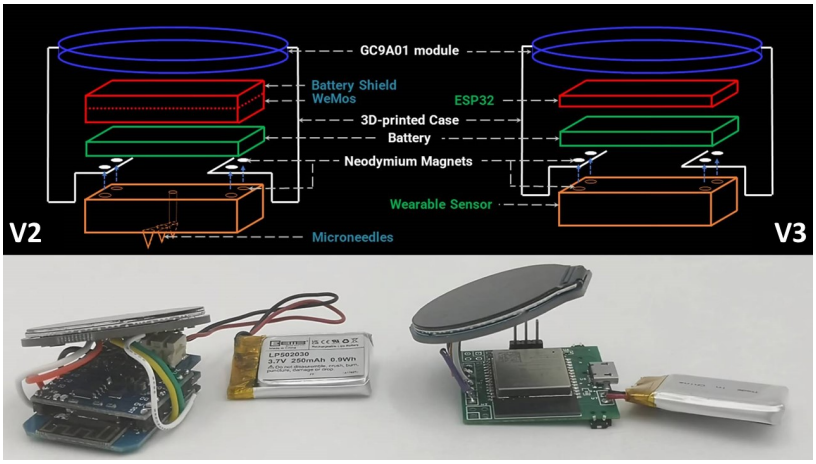

Figure 2.17: Hardware architecture comparison between the second and third versions of the BioWatch.

2.3 Software Development

2.3.1 Technical Specifications

The GC9A01 is programmed in C++. The Adafruit GFX library is involved in designing the whole screen in color. The library provides standard syntax and graphics functions for LCD and OLED displays and LED matrices. An open-source code allows the display of a classic watch face with three hands on the first version. For the second and third versions of the BioWatch, a code was specifically developed to meet the identified needs.

Resorting to a Network Time Protocol (NTP) permits setting the watch on time. The NTP allows the ESP8266 to request and receive the Coordinated Universal Time (UTC), depending on the location. Connecting with a local WiFi network automatically synchronizes the smartwatch's clock on computer networks.

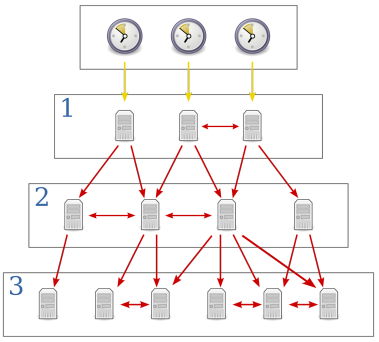

Figure 2.18: Synchronization of atomic or radio clocks in local and global networks with NTP.

2.3.2 User Needs Analysis

A needs analysis phase was carried out regarding the watch interface design. This work aims to identify the adoption factors of a smartwatch with integrated biosensors and to design a data visualization interface that best meets user needs. This area of research is part of BioWatch's overall vision to facilitate integrating and adopting biosensors in smartwatches to improve user health.

Five different pieces of information should appear on the screen. These elements were identified in collaboration with the PKvitality design team. PKvitality is a technology company developing the first CGM smartwatch. The design team consulted with many professionals and patients to identify and prioritize the information displayed on the watch. Five different pieces of information emerged:

- the time of day in *hh:mm:ss* format;
- the date in *jj-mm* format;

- the last measured value of the biomarker level, allowing a rapid understanding of the actual glycemia level;
- a visual indicator system to quickly read whether the data shows hypo- or hyperglycemia;
- a prediction of the next measured data to better identify the evolution trend.

A final-users consultation was conducted to validate and deepen the conclusions discussed. Several populations were considered for the study. We ultimately consulted people with diabetes for several reasons: these patients are familiar with biosensors, glycemic variations are frequent, and the need for effective monitoring is crucial. In addition, diabetic patients use CGMs every day and are strongly impacted in their daily lives. They are thus a source of proposals for improving CGMs, as demonstrated by the community's online forums and conversations. Other populations who have never or rarely been confronted with biosensors can also benefit from the frequent use of a biosensor-enabled smartwatch. These include high-level athletes and patients suffering from lactic acidosis for lactate in particular. However, these people unfamiliar with biosensors need help to fully discern the added value of a wearable biosensor for their use case. Five French volunteers prone to Type 1 diabetes participated in the need analysis. Three adult men, one woman, and one child expressed their expectations of a CGM smartwatch interface. The identified expectations are summarized below:

- 60-90 minutes of data history displayed on the watch screen was optimal;
- most commercial CGMs have a measurement update frequency of one minute. The subjects all expressed satisfaction with this update frequency;
- users would like the unit of concentration to be expressed in mg/dL. French patients are more familiar with this unit;
- a color code or threshold system seems essential to them to facilitate reading during a hyperglycemic or hypoglycemic crisis;

- the graph range, limited by the biosensor's performance, is ideally between 30mg/dL and 250mg/dL - according to their already experienced hyperglycemic and hypoglycemic crises.

Analyzing patients' needs allowed to define precise specifications for developing the BioWatch interface.

2.3.3 Design study

Four different designs resulted from the specifications and needs analysis. Each of them has been schematized in figure 2.19. They were presented to a group of twenty-five students who judged the designs, and each chose the design they thought the most appropriate for a CGM smartwatch. Design (1) got four votes, design (2) got twelve votes, design (3) got zero votes, and design (4) got nine votes.

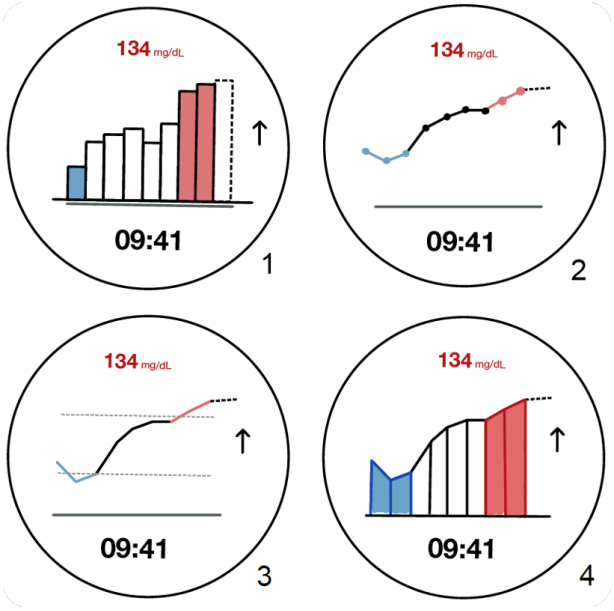

Figure 2.19: Designs presented to 24 subjects.

Design (2) was therefore implemented. The functions of the GFX library, such as drawPixel and drawLine, permit the drawn sketch's concretion on the watch display.

2.3.4 Implementation

The GC9A01 display is 240*240 pixels wide. The data history graph spans a central rectangle of 190 pixels on

the x-axis by 140 pixels on the y-axis, from pixel (25;190) to pixel (215;50). Eighteen data points are displayed every 10 pixels on the x-axis. Based on a left-to-right reading, the most recent measured point is on the right of the graph (abscissa 205) and the oldest on the left (abscissa 25). A nineteenth point is displayed at the x-axis 215. An algorithm predicts the next concentration according to the last four measured values.

When the glucose level drops below 70mg/dL (hypoglycemia threshold), the resulting point and the associated segment appear in blue (instead of white). Conversely, when the level exceeds 120mg/dL (hyperglycemia threshold), these graphic elements are colored red(figure 2.20). The last measured value - displayed at the top of the screen - also changes color under the same conditions.

Every five minutes, the data is updated. The "point" element n ordinate is assigned to the "point" element n+1. The element n = 0 gets the new value, and a new prediction value is calculated. This time of 5 minutes is much longer than the patient needs. However, this frequency simplifies the screen's design by counting only 18 data points. Now that the first software is operational, future work will multiply this number by 5 to allow an update frequency of one minute and a history of 90 minutes.

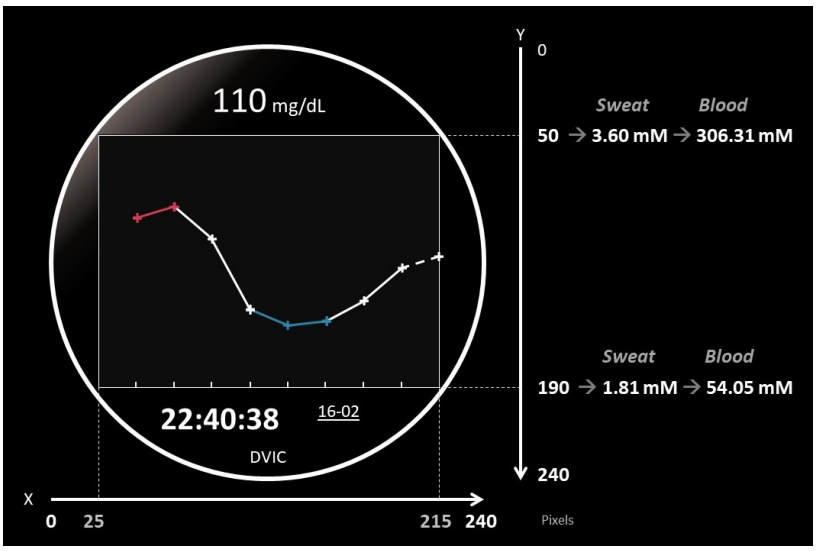

Figure 2.20: Design of the BioWatch V2 and V3 display.

The interface is adapted to the blood glucose concentrations of people with diabetes. However, the interface is, by design, easily transposable to other concentration scales. The code provides for the automatic adaptation of the graph by editing the minimum and maximum values through a simple cross-product. The refresh rate of the last displayed measurement and the graph is also easily adjustable. The history covered by the graph is also editable. An animation welcomes the user when switching on the BioWatch.

2.3.5 User Experience

A user study was conducted with three diabetic patients (2 men and one woman). The objective is to evaluate the user experience of the BioWatch as a smartwatch and CGM. Participants held the BioWatch for two hours. They could perform various household chores and activities at home during this time. The interface displays simulated data throughout the test period. The refresh rate is set at 2 minutes, and the data history is set at 40 minutes. We conducted the study with the second version of the BioWatch. A non-invasive microneedle biosensor module was placed under the smartwatch.

Figure 2.21: The BioWatch worn by a subject

Two of the three subjects reported that the smartwatch case was too voluminous from an aesthetic point of view but relatively comfortable. All participants expressed being slightly bothered by the microneedles. Each of them is globally satisfied with the user interface.

On the monitoring aspect, the three patients are moderately or somewhat satisfied. The history of the evolution of 40 minutes seems adequate to them regarding the size of the wearable screen. All were also satisfied with the two-minute refresh rate, but 2 preferred one.

All would rather wear a smartwatch-like CGM similar to the BioWatch than their current CGM (Freestyle Libre 3 for each). The points they would like to be improved to buy such a device are aesthetics, connectivity (basic features of a smartwatch), interactivity (touch screen), screen resolution, and a more modern user interface. Participants also expressed that they sometimes failed to anticipate hypo- and hyperglycemia attacks with BioWatch, as they did not watch the screen regularly enough. A suggested solution is to incorporate a vibratory motor triggered in case of crisis.

2.4 Wireless connection with a wearable glucose biosensor

A proof-of-concept for a non-invasive glucose biosensor has been assembled. The autonomous system measures the glucose concentration in sweat. A wireless connection between the biosensor and the second version of the BioWatch has been established. This work results in the BioWatch's connectivity with sensors not physically integrated into the watch. The on-wrist data visualization platform is thus compatible with sensors in different body locations.

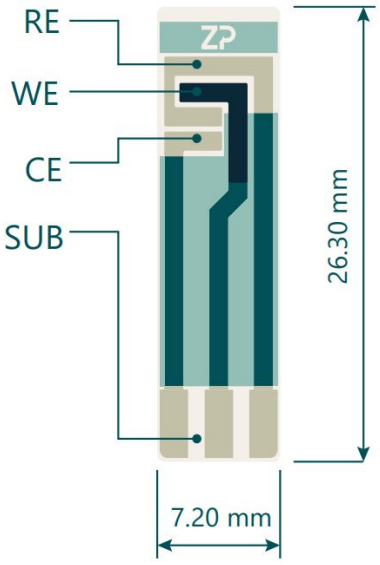

Figure 2.22: Screen-printed electrodes, 24.4 millimeters long, from Zimmer&Peacock. The GOx enzyme is placed on the end of the WE. The RE surrounds the functionalized WE surface. From [103]

2.4.1 Wearable Sensing System Assembly

The sweat glucose monitoring system comprises a biosensor functionalized on screen-printed electrodes (SPEs), a microfluidic patch, and signal acquisition electronics sourced from Zeammer&Peacock (ZP).

The patch is made up of several self-adhesive plastic elements. Once assembled on SPEs, the pre-cut microfluidic

channels convey sweat to the sensor's active surface. The sweat patch collector ensures a controlled continuous flow of sweat to the SPEs.

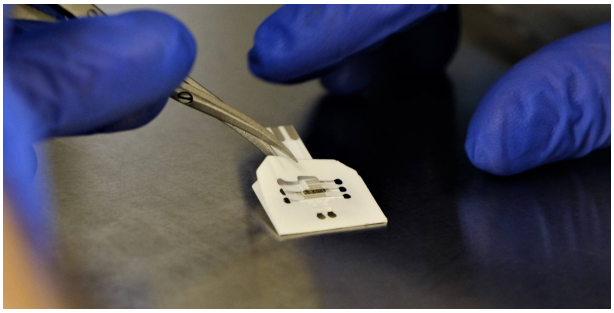

Figure 2.23: Assembling the sweat collection patch on a glucose biosensor.

The glucose biosensor adheres to the conventional three-electrodes cell configuration, including the reference (RE), counter (CE), and working electrodes (WE)(2.22). This three-electrode system is screen-printed on a substrate [104]. SPEs are made with thick-film deposition [105]. This process allows simple, rapid, and inexpensive production of biosensors [106]. Materials printed on ZP glucose sensor are silver/silver chloride for the RE and CE and platinum for the WE [107]. The WE encompasses glucose oxidase (GOx), an oxidoreductase enzyme that facilitates the oxidation of glucose into hydrogen peroxide (H_2O_2) (2.1) [108]. The charges released during H_2O_2 reduction flow from the WE to the RE (2.2).

$$C_6H_{12}O_6 + O_2 \leftrightharpoons C_6H_{10}O_6 + H_2O_2 \quad (2.1)$$

$$H_2O_2 \leftrightharpoons O_2 + 2H^+ + 2e^- \quad (2.2)$$

Figure 2.24: (2.1) Glucose oxidation into glucono-δ-lactone and hydrogen peroxide and (2.2) hydrogen peroxide oxidation [109].

The sensor is pluggable on a flexible, stamp-sized, electrochemical sensor platform known as the ec-Flex(2.26) [110]. This platform incorporates an open-circuit potentiostat, enabling continuous steady-state chronoamperometric measurements [111]. The integrated Bluetooth circuitry achieves data transmission through Bluetooth low energy (BLE). A slim, flexible lithium polymer battery is attached to the ec-Flex, discreetly disposed between the skin and the bendable electronic board(2.27). The battery lifetime is approximately 8 hours [112]. All the equipment was purchased from Zimmer&Peacock

website [113].

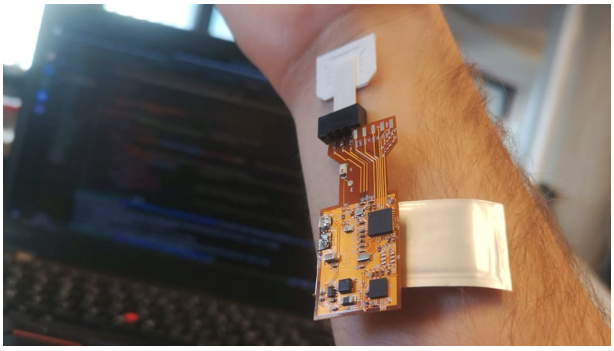

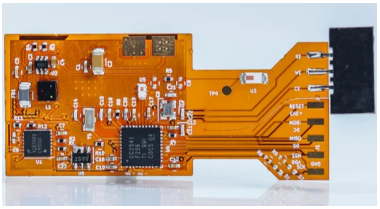

Figure 2.25: The ec-Flex from Zimmer&Peacock.

Figure 2.26: The wearable non-invasive glucose biosensor disposed on a forearm.

The selection of the ec-Flex board is informed by its ability to serve as a rapid prototype platform, apt for demonstrating proof of concept. Moreover, BLE ensures high autonomy for low-frequency monitoring, making it well-suited for acquiring electrochemical data on the skin, given the relatively gradual evolution of sweat biomarker concentrations. BLE has shown substantial promise in the wearables industry and is the prevalent technology for wirelessly transmitting analyzed data, alongside near-field communication (NFC) [114, 115]. In addition, SPEs are a promising tool for constructing portable analytical devices due to their small size [116].

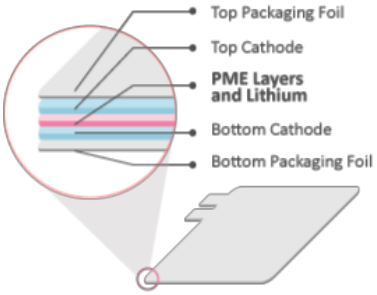

Figure 2.27: Slim, flexible battery made by BrightVolt. From [112]

2.4.2 Data Specifications

Data from the ec-Flex are received by a laptop, which then interprets and forwards the data to the WeMos. All data is logged in a local database. The ec-Flex data is transmitted in byte array format, with each byte array containing four values: an ID, a timer, temperature, and an electrochemical sensor readout. Given the relatively slow variation in glucose concentration in sweat, high-frequency data acquisition is unnecessary. The ec-Flex is configured to transmit data every second. Real-time data display on the smartwatch is desired, with a target time lag of less than 5 seconds. The 8-hour battery lifespan limits the system's autonomy. The maximum data volume is approximately 30,000-byte arrays, equating to 120,000 usable values. The local database must accom-

modate three times this volume, totaling 480,000 values, to support potential medical diagnostic applications in the project's future scope.

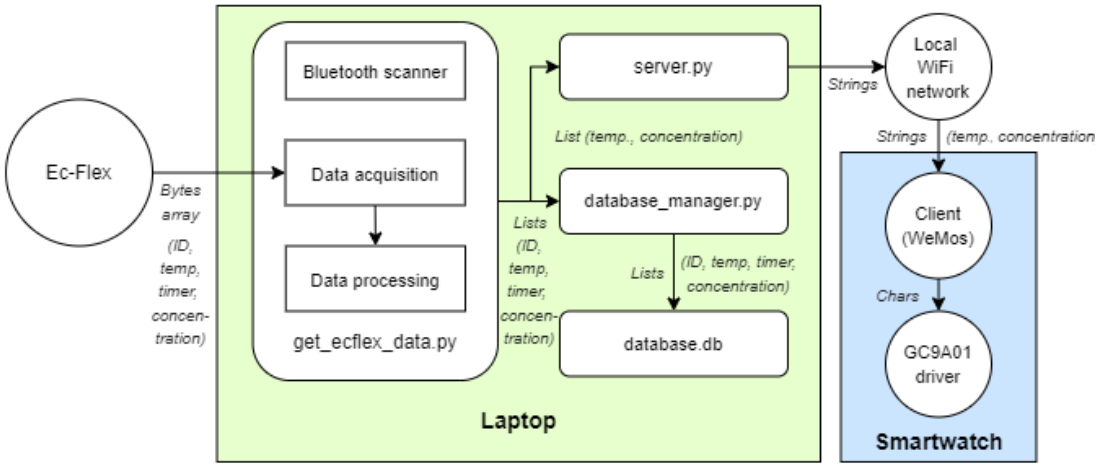

Figure 2.28: Deployment diagram of the wireless communication solution between the ec-Flex, the laptop and the WeMos microcontroller.

The ec-Flex functions as a server, while the laptop assumes the role of the client [111]. The initial code block entails a Bluetooth scanner algorithm for filtering purposes. The server-client connection is established using the bleak library [117]. The BLE stack utilizes the generic attribute profile [118]. A service encompasses data and associated functionalities to fulfill a specific function. Characteristics are the data components within services. Specifically, the "Handle 17 – Sensor command" characteristic within the "Vendor service" contains live data. Variables required to interpret the electrochemical sensor readout are obtained from other characteristics:

- D0: Analog-to-Digital Converter (ADC) resolution;
- X0: virtual ground level;
- D1: current-to-voltage amplification;
- N1: Scale factor for current;
- N2: Scale-factor for non-offset linear conversion.

2.4.3 Data Acquisition

Data is encoded in ASCII format. After hexadecimal decoding, the byte array is divided into four parts. The

initial two bytes represent the ID, the subsequent two denote the timer, the third pair signifies the temperature value, and the final byte indicates the biosensor ADC value. Notably, the byte order must be reversed (big-endian to little-endian) for decimal conversion.

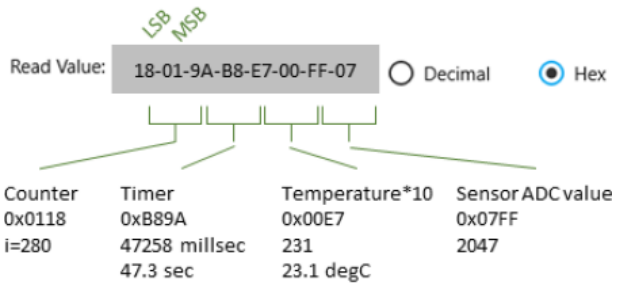

Figure 2.29: Bytes structure sent by the ec-Flex.

Glucose concentration is deduced from the sensor ADC value using specific formulas [111]:

$$V_{out} = \frac{N_0}{D_0} \times ADC - \frac{X_0}{100} \tag{2.3}$$

$$I = -100 \times \frac{N_1}{D_1} \times V_{out} \tag{2.4}$$

$$C_g = \frac{I}{N_2} \tag{2.5}$$

The system conveys temperature and glucose concentration data as a string to the WeMos. An HTTP persistent connection is established between the laptop (TCP server) and ESP8266 (TCP client). The server program is scripted in Python and operates in parallel using multithreading to send real-time data to the client. Flask micro web framework is employed to configure the sending application with a concise script [119]. The client program, written in C++ on the Arduino IDE, facilitates code upload to the microcontroller. The WeMos operates in station mode, obtaining an IP address from the connected wireless router. Serial communication between the WeMos and the laptop is established via the Arduino IDE serial monitor. Arduino-uploaded code ensures the data is displayed in almost real-time.

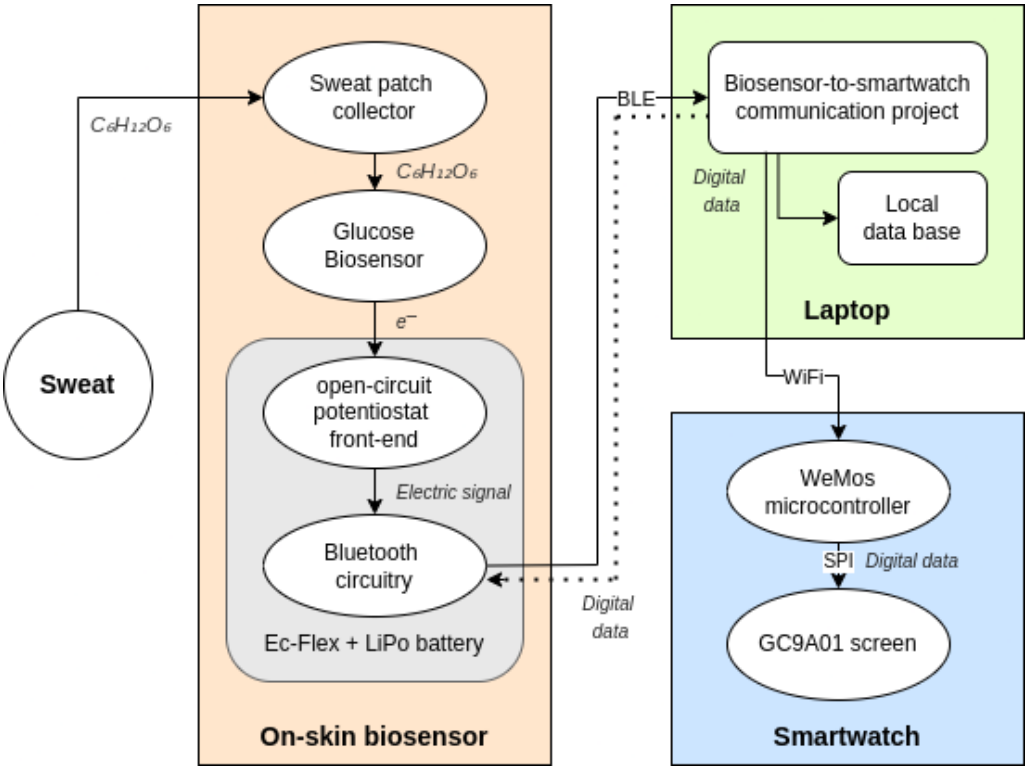

Figure 2.30: Functional diagram of the wireless communication between the biosensor and the smartwatch.

Each byte sent by BLE is stored in a database on the computer. The database schema adopts a straightforward table structure with four columns: ID, timer, temperature, and glucose concentration. A Python program, utilizing the SQLite3 Python module [120], manages the database, with multithreading enabling the main program to record newly acquired data in a database.db file.

Additional scripts facilitate the swift retrieval of BLE connection characteristic addresses essential for the main program. Additionally, an Arduino script aids in identifying available Wi-Fi networks for the HTTP connection, providing information on SSID and RSSI for each network.

All the code is available on the BioWatch GitHub repository [79].

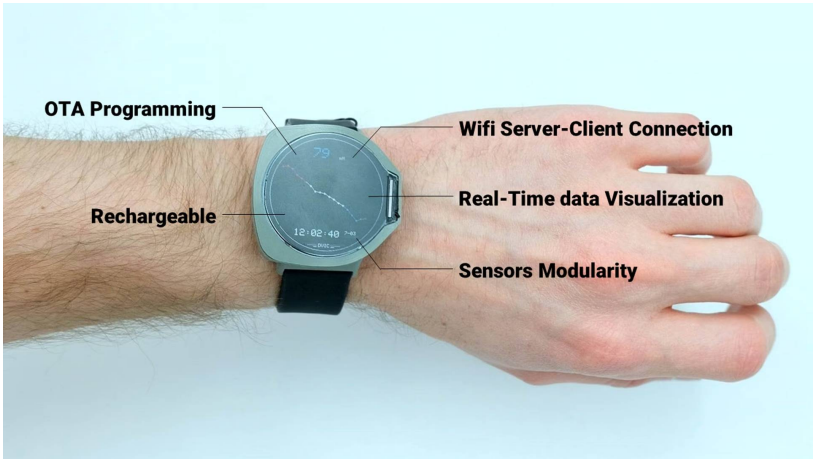

Figure 2.31: Various connectivity features implemented in the BioWatch.

2.5 Future works

The BioWatch has several limitations. First, the V3 still needs to be functional. The PCB with a potentiostat circuit was designed but not printed. The physical connection between the biosensor modules and the BioWatch is therefore inoperative. Future work is, therefore, to develop this electronic circuit. Preliminary tests with prototypes based on the LMP91000 and a commercial biosensor are necessary to validate the proper functioning of the circuit before printing. In the second step, we will have to merge the two PCBs. This step requires a robust optimization of the circuit. A single PCB significantly contributes to embedded electronics in smartwatches for biosensors. Such a solution design requires significant research and development microelectronics work. Another limitation is the single-channel acquisition. The proof of concept developed allows the display of a single monitored biological data. Designing a new interface with several data presented in parallel is necessary for multi-analyte proof-of-concept. BioWatch connectivity is also limited. Future work is required to implement new features similar to the marketed smartwatches. These features include connecting with the user's smartphone, communication functions such as viewing or sending messages, and integrating a touch screen to interact with the data easily. The monitored data can be backed up and subsequently consulted on a mobile or web application by the user or a healthcare

professional. The user study also revealed the need to integrate a vibration functionality to signal abnormal biomarker levels. The watch's autonomy must also be increased throughout the day. Additional efforts are needed to improve the user experience of the developed CGM smartwatch from a user-centric conception perspective.

2.6 Conclusion

Technical advances in biosensors enable the detection of a wide range of molecular biomarkers, potentially surpassing existing medical wearables. Driven by smartwatch technology, wearable biosensors have the potential to concretize comprehensive health monitoring for chronically ill patients and, in a more distant future, for the general public. The BioWatch represents a significant step forward in integrating biosensors into smartwatches. This research endeavor has striven to bridge the gap between cutting-edge biosensing technology and a popular wearable device, smartwatches.

The primary contributions of this work include the fabrication of the first smartwatch prototype for wearable biosensors co-development and integration. Considering the importance of user-centric design for adopting biosensors into wearables, we provide a user study of diabetes people's experience with the BioWatch.

Certain limitations need to be addressed in future research. The functionality of the third BioWatch version remains incomplete, necessitating further work on the electronic circuit and PCB optimization. Additionally, the BioWatch only supports single-channel acquisition, requiring future enhancements to accommodate multi-analyte proof-of-concept.

In the broader context, integrating biosensors into smartwatches opens up promising possibilities for the future of healthcare. The seamless amalgamation of biosensing technology with wearable devices can revolutionize real-time health monitoring and data visualization, ul-

timately empowering individuals and healthcare professionals to make informed decisions regarding their well-being. As research advances in this field, the vision of comprehensive and user-friendly health monitoring through smartwatches integrated with biosensors moves closer to becoming a reality.

A Microneedle Lactate Biosensor For The BioWatch

3

3.1 Introduction

Healthcare applications of lactate monitoring

The monitoring of lactate levels holds significant importance in diagnosing and assessing various health conditions [121], including lactate acidosis and situations characterized by oxygen deficit, where lactate levels exceed accepted norms [122]. These applications span diverse domains such as military and high-risk personnel healthcare, clinical emergencies, sports medicine, general medical practice, and the food industry [123, 124]. For instance, insufficient oxygen supply during childbirth can result in fetal acidosis marked by increased lactate levels in the fetal blood, with lactate and pH levels as crucial indicators of distress during labor [125]. Furthermore, heightened lactate levels may signal bacterial or fungal infections in enclosed body cavities such as joints, meninges, or pleura [126]. In cancer cells and tumors, lactate is pivotal in acidifying the microenvironment, potentially contributing to tumor development [127]. Lactate also holds significance in assessing brain metabolism, offering insights into cerebral stroke or traumatic brain injuries [128]. However, relying solely on laboratory-based testing systems falls short of effectively diagnosing and monitoring these life-threatening conditions.

Sports applications of lactate monitoring

Although many medical applications, the demand for lactate monitoring solutions comes mainly from the sports domain. Lactate monitoring is instrumental in gauging training intensity and evaluating an athlete's endurance [129, 130]. Exercise-induced muscle fatigue is a reversible loss of muscle force (or muscle contractility) during work over time [131]. Human *in vivo* studies

have demonstrated conspicuous concomitances between muscle lactate and proton concentrations, cellular pH, and muscle fatigue [132, 133]. Whether these concomitances reflect cause-effect relationships is still debated. Lactate has not been shown to cause muscle fatigue directly. Muscle lactate is, with interleukin-6 [134], a well-known and relevant biomarker of exercise-induced muscle fatigue [135–137]. Understanding and monitoring lactate levels allows athletes to adapt their training plans, optimize their workouts, prevent overtraining, and ultimately enhance their performance in their respective sports. Coaches and sports scientists interpret lactate data accurately and design training programs tailored to their needs and goals [129, 138].

Currently, lactate detection is mainly performed using blood sampling analyzers [139]. The most known hand-held blood lactate analyzers are the Lactate Pro, the Lactate Pro2, the Lactate Scout+, the Xpress, and the Edge [140]. Although reliable and accurate measurements are performed with such devices [140, 141], athletes must stop moving for blood collection from their fingertips or earlobes. Moreover, for lactate and any biomarkers, blood sampling is uncomfortable for users, cannot be used for continuous measurement, and is relatively expensive.

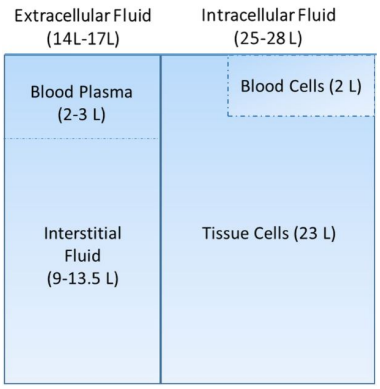

Figure 3.1: Distribution of water in the human body showing the approximate volume of blood plasma and ISF in the extracellular fluid compartment, and the volume of tissue and blood cells in the intracellular fluid compartment. From [142]

Microneedles technology for lactate monitoring

In recent years, developing non-invasive or minimally-invasive biosensors for continuous lactate monitoring has raised strong interest in wellness and sports applications. The two body fluids mainly considered by researchers to carry out these non-invasive measurements are sweat [143] and ISF [144]. For detection in ISF, recent technology has proven its potential: microneedles [145]. Microneedles have been developed for various applications, including drug delivery, biosensing, and vaccination. They offer a minimally-invasive and user-friendly alternative to conventional needles, causing less pain and lower tissue damage [146]. Microneedles are fabricated using different techniques and materials, resulting in various types such as solid, dissolving, coated,

and hollow microneedles [147]. In recent years, 3D printing has emerged as a promising technique for fabricating microneedle arrays, enabling point-of-care biosensing applications [146]. Additionally, microfluidic technology has been used to control the porosity of polylactic acid porous microneedles, allowing for adjustable ISF extraction efficiency [148]. Due to the small dimensions of microneedles (less than 1 mm in length), they can penetrate the stratum corneum without reaching deep into the subcutaneous tissue, unlike the needle sensors used in commercially available CGM devices [149].

The inherent biological attributes of ISF complement its practical advantages. The molecular weight cutoff between blood and ISF is high, approximately 1 MDa, making ISF a rich biomarkers biofluid [95]. Concentrations are similar to plasma concentrations for low molecular weight species, and the blood-to-ISF lag time is between 5 to 15 minutes [95]. The commercial maturity of biodetection in ISF is asserted yearly. **new biomarkers such as lactate could be monitored non-invasively with the emergence of microneedles biosensors** [150].

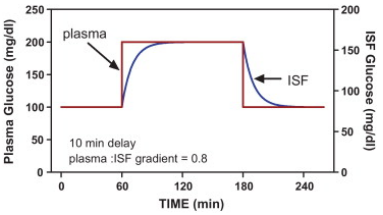

Figure 3.2: The lag time of glucose concentrations in the ISF is around 10 minutes compared with plasma concentrations. From [151]

The work presented in this section aims to develop a microneedle-based lactate biosensor. The biosensor presented is an enzymatic sensor. This project consists of several conception stages. The programming of a potentiostat development board, the biosensor functionalization, and the design and 3D printing of a microneedle module. Each development stage is illustrated by the electrochemical concepts involved in the design and operation of the biosensor.

Complementary works accompany this technical development. Firstly, we provide an exhaustive literature review on lactate pharmacology in the human body and lactic concentrations in ISF during physical exercise. This state-of-the-art analysis aims to evaluate the relevance of lactate monitoring in dermal ISF for muscle fatigue quantification. Secondly, we present an educational application illustrating the microneedle biosensor working at the molecular scale. The platform developed is the first immersive 3D app for interactive learning of the

basic principles of biosensors.

3.2 Lactate pharmacology for minimally-invasive biosensor development

Understanding biomarkers' behavior in the organism is a prerequisite for biological detection research [152]. Clinical qualification is the evidentiary process of linking a biomarker with biological processes and clinical endpoints [153]. Clinicians evaluate the magnitude of the reason for the clinical cause of this biomarker production and establish a diagnosis. Studying biomarkers pharmacology is therefore essential before designing wearable biosensors.

A considerable body of clinical research has been devoted to glucose pharmacology in human ISF [154]. Although the state of the art is relatively well established for lactate as well [95], the lactic concentrations in the dermal ISF, in particular, remain relatively understudied. However, such clinical knowledge arouses growing interest, as biomonitoring technologies become increasingly mature and able to measure lactate concentrations in the skin painlessly.

The following work reviews the literature on lactate pharmacokinetics in the ISF during physical exercise. This state of knowledge aims to **highlight the relevance or irrelevance of dermal ISF as a medium for physical activity-induced lactate monitoring** and areas of persistent uncertainty.

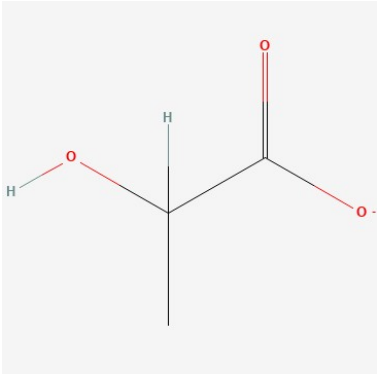

Figure 3.3: 2D Chemical Structure Depiction of Lactate [155]

3.2.1 Definitions

D-lactic acid & L-lactic acid

Lactic acid is a natural organic acid that can take the form of two enantiomers: *l-lactic acid* and *d-lactic acid*. **L-lactic acid is an endogenous compound involved in human energy metabolism** [156]. Tissue sources of l-lactate

production include *erythrocytes*[1] , *hepatocytes*[2] , *skeletal myocytes*[3] , skin, and *astrocytes*[4] [158, 159]. On the other hand, d-lactic acid is produced in some less relevant metabolic pathways or by microorganism strains [160]. Lactic acid bacteria produce lactic acid in the small intestine and colon [161, 162]. **Blood contains approximately 100 times more l-lactate than d-lactate** [129, 163]. The pathological significance of lactate is almost entirely confined to the l-lactate isoform [164]. It is the isoform routinely measured at the point of care [165] and in the laboratory [166].

1: Erythrocytes are red blood cells.

2: Hepatocytes are the chief functional cells of the liver[157].

3: Myocytes are muscle cells.

4: Astrocytes are a sub-type of cells in the central nervous system

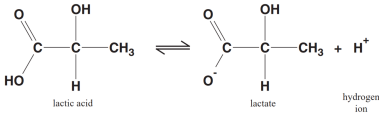

Figure 3.4: The dissociation of lactic acid. From [158]

Lactate & Lactic acid

Lactate is a hydroxy monocarboxylic acid anion [155]. The lactic acid's conjugate base arises from the carboxy group's deprotonation [155, 167]. Lactic acid pKa [5] (3.86 [155]) is lower than physiological pH values [6] [169, 170]. Consequently, **lactic acid metabolized is dissociated at more than 99% into lactate and H^+ ions** [169], like other organic acids of intermediate metabolism [167]. The interchangeability of lactic acid and lactate terms in physiology is thus relatively justified.

5: pKa is the negative logarithm of the acid dissociation constant. The lower the value of pKa, the stronger the acid and the greater its ability to donate its protons.

6: The human body pH ranges between 7.35 to 7.45 under normal conditions [168].

3.2.2 Lactate metabolism & Cori cycle

Aerobic respiration & Anaerobic respiration

During rest and light physical activity, oxygen supply to cells is sufficient for *aerobic respiration*. Aerobic respiration is a cellular metabolism process by which cells break down carbohydrates and lipids to generate *adenosine triphosphate*[7] (ATP) molecules. Glucose molecules are formed from glycogen in the cell or supplied by the GLUT4 transporter from blood [173]. Glucose is broken down during the glycolysis process. *Nicotinamide adenine dinucleotide* (NAD+) co-enzyme catalyzes this reaction in the cytoplasm. The intermediate metabolite *pyruvate* is produced. If oxygen is abundant in the cell, pyruvate can enter the mitochondria, generating 32 to 38 ATP. Intense exercises cause cellular hypoxia and lead to anaerobic metabolism. *Anaerobic respiration* is the

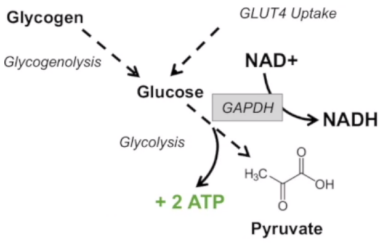

Figure 3.5: Pyruvate production in cells from glucose.

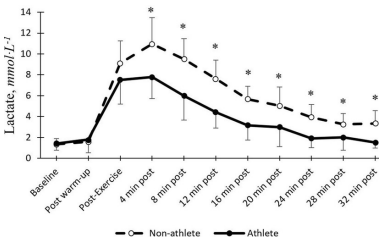

Figure 3.6: Blood lactate response in athletes vs. non-athletes. *Statistically significant difference between athletes vs. non-athletes (adjusted $p < 0.005$). From [171]

process by which skeletal muscle cells produce energy without oxygen. The *Cori cycle*, also known as the Lactic acid cycle, describes the metabolic pathway of lactic acid produced during anaerobic metabolism by skeletal muscle cells [174]. Instead of entering the mitochondrial matrix, excess pyruvate is catalyzed with Nicotinamide adenine dinucleotide (NADH) by lactate dehydrogenase (LDH) enzyme into lactic acid. LDH has a greater binding affinity for l-lactate than d-lactate [167]. D-lactate is, when present, metabolized at a slower rate.

Muscle lactate release

High lactic acid production can cause lactic acid acidosis[8] in muscle cells [180, 181]. The monocarboxylate transporter MCT1[9] avoid acidosis by evacuating lactic acid from the muscle cell to the blood [183, 184]. Lactate is buffered in plasma by bicarbonate of soda ($NaHCO_3$) [158]. **Lactic acid accumulates in contracting muscle and blood, beginning around 50-70% of the maximal O_2 uptake**, well before the aerobic capacity is fully utilized [185]. The predominant explanation is that lactate production during submaximal dynamic exercise is not O_2 dependent [186].

Lactate fate in the organism

Lactate produced during exercise muscle is distributed unevenly throughout the body's different compartments [178]. The anaerobic component of cellular metabolism can be theoretically assessed by measuring lactic flux at the cellular level or the level of the isolated muscle [187]. At the whole organism level, blood measurements are more complex to be relevantly interpreted as a muscle fatigue indicator due to the actions of different bodies on the lactic flux, the action of unused muscles, and the multicompartmental diffusion of lactate [187]. Different compartmental models have been formulated to predict blood lactate concentration ($[La^-]_{blo}$) [188–194]. Although some show promising results, these models have limitations. They usually include many assumptions not applicable to continuous monitoring, such as when the maximum post-exercise $[La^-]_{blo}$ will be

7: ATP is the energy source for use and storage at the cellular level [172].

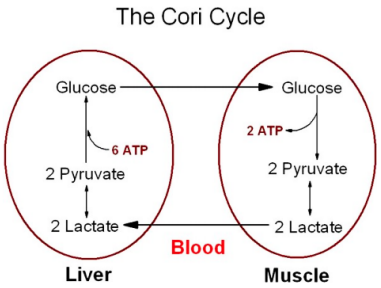

Figure 3.7: Corri cycle schematic overview. From [175].

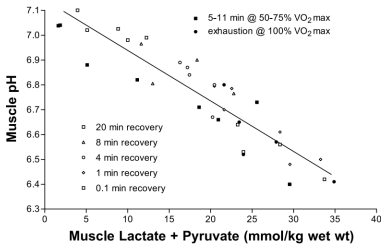

Figure 3.8: Figure redrawn from data from Sahlin et al. [176] (Figs. 1 and 2, p. 46), showing the linear relationship between the sum of muscle lactate and pyruvate vs. muscle pH. Data are combined from different exercise intensities and different recovery durations after exercise to exhaustion. From [177].

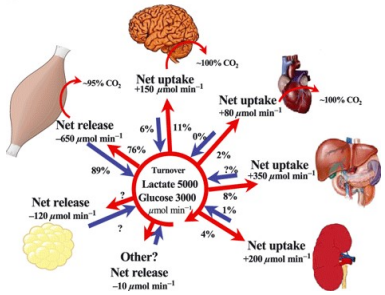

Figure 3.9: Scheme of tissue contributions to systemic lactate turnover in healthy humans during moderate intensity exercise. From [178]

reached, a glycogen fixed concentration, or specific stimulation intensities or durations. Although they do not make it possible to formulate complete models, the advances made in recent years provide answers regarding the distribution of lactate in the different compartments of the body.

3.2.3 Lactate pharmacokinetics during exercise

Lactate produced during exercise muscle is distributed unevenly throughout the body's different compartments [178]. The anaerobic component of cellular metabolism can be theoretically assessed by measuring lactic flux at the cellular level or the level of the isolated muscle [187]. At the whole organism level, blood measurements are more complex to be relevantly interpreted as a muscle fatigue indicator due to the actions of different bodies on the lactic flux, the action of unused muscles, and the multicompartmental diffusion of lactate [187]. Different compartmental models have been formulated to predict blood lactate concentration ($[La^-]_{blo}$) [188–194]. Although some show promising results, these models have limitations. They usually include many assumptions not applicable to continuous monitoring, such as when the maximum post-exercise $[La^-]_{blo}$ will be reached, a glycogen fixed concentration, or specific stimulation intensities or durations. Although they do not make it possible to formulate complete models, the advances made in recent years provide answers regarding the distribution of lactate in the different compartments of the body.

Muscle versus blood lactate concentrations

$[La^-]_{blo}$ results from global lactate appearance and disappearance, not only the lactate appearance and disappearance of the stimulated muscle fibers [132, 195]. The lactate transport from the active muscle to the blood, which depends on the concentration gradient, also plays a role [132]. Despite the complexity of the phenomena to be taken into consideration, numerous pieces of evidence

8: Lactic acidosis is defined as a blood lactate concentration of 5 mmol/L and a pH lower than 7.35 [179].

9: Monocarboxylate transporters (MCTs) catalyze the proton-linked transport of monocarboxylates such as L-lactate, pyruvate, and the ketone bodies across the plasma membrane [182].

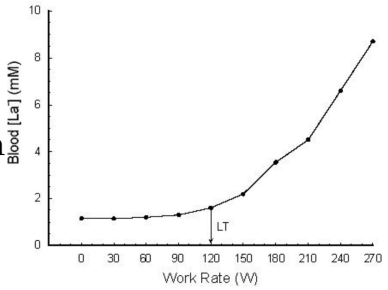

Figure 3.10: A typical [La-]b response to a progressive, incremental exercise test. LT represents the "lactate threshold." These are whole blood measurements corrected for water content. From [129]

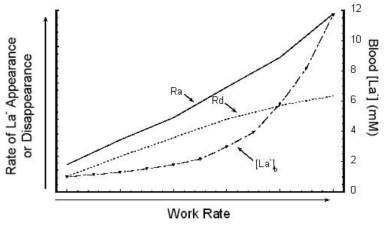

Figure 3.11: Schematic view of Lactate rate of appearance (Ra), Lactate rate of disappearance (Rd), and resulting $[La^-]_{blo}$ during progressive, incremental exercise. From [195]

demonstrate that **active muscle lactate concentration ($[La^-]_{mus}$) presents similar patterns to those of $[La^-]_{blo}$** [196–199].

Whole blood versus plasma lactate concentrations

Several studies show an inhomogeneous distribution of lactate in blood during graded exercise [200–203]. According to their membrane potential, the erythrocytes' intracellular concentration is lower than the plasma lactate concentration ($[La^-]_{pla}$) [129, 202, 204]. **Consequently, whole $[La^-]_{blo}$ must be differentiated from $[La^-]_{pla}$**. The whole blood-plasma lactate concentration ratio might vary from 63% to 81% depending on plasma water content and hematocrit[10] [129]. **$[La^-]_{pla}$ is, around 1.5 times higher than whole $[La^-]_{blo}$ at rest**[11] [207–209]. This ratio increases during rapid and graded exercise-induced lactate releases [200, 204]. This distinction is a significant issue for blood lactate measurements. Indeed, different lactate analyzers measure plasma or whole blood lactate concentration. **Which concentration is measured by point-of-care devices could be unclear** [129]. $[La^-]_{pla}$ is traditionally measured in central laboratories.

Arterial versus capillary blood lactate concentrations

Arterial blood is the standard sample for laboratory lactate measurement [210]. It gives a reliable indication of global appearance and disappearance [211]. **At rest, arterial lactate and capillary lactate are weakly correlated** [209]. Several studies demonstrate that capillary plasma lactate concentration ($[La^-]_{cap}$) and hand-held point-of-care (POC) device measurements are significantly higher than arterial plasma lactate concentration ($[La^-]_{art}$) and its measurements in laboratory [212–214]. The magnitude of this bias varies between studies [211]. Unlike well-validated central laboratory equipment, hand-held POC devices do not provide sufficiently relevant clinical data to draw medical diagnoses[215, 216]. **However, correlation between $[La^-]_{art}$ and $[La^-]_{cap}$ increases during physical exercise** [209]. Although capillary blood samples for in-hospital medical diagnostics remain debated,

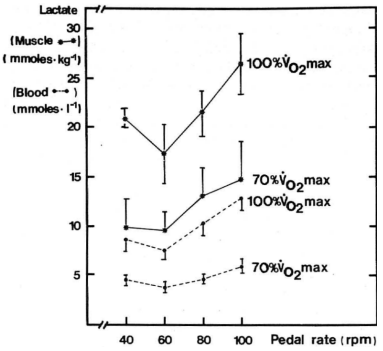

Figure 3.12: $[La^-]_{mus}$ (stars) and $[La^-]_{blo}$ (dots) for submaximal (70%Vo2max) and maximal (100%Vo2max) exercise intensity in six healthy male subjects during bicycling exercises. From [196]

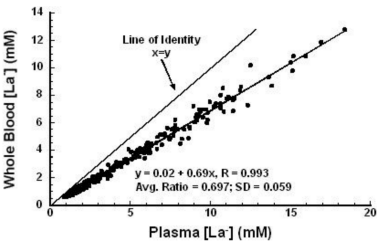

Figure 3.13: Whole $[La^-]_{blo}$ versus corresponding $[La^-]_{pla}$. SD: standard deviation of $[La^-]_{blo}$ to $[La^-]_{pla}$ ratio. N = 324 blood samples. From [129]

10: The hematocrit is the volume percentage of red blood cells in blood

11: In comparison, plasma glucose values are about 10% - 15% higher than whole blood when the hematocrit is normal [205, 206].

capillary lactate measurements are consistently usable for sports training applications [209, 217, 218].

Absolute capillary blood lactate concentrations versus portable analyzers measurements during exercise

The most important study on commercialized portable blood lactate analyzers since 2015 was led by J. M. Bonaventura et al. [219]. They realized a comparative study on five hand-held blood lactate analyzers. They tested the devices on venous blood samples. **The devices' reliability was generally lower than 0.5 mM for concentrations of 1.0 to 10 mM**. For all five portable analyzers, the analytical error within a brand was much smaller than the biological variation in venous blood lactate. **Compared with a criterion blood lactate analyzer, all portable analyzers tend to under-read (i.e., a negative bias), particularly evident at the highest concentrations (15 to 23 mM)** [219, 220].

Capillary blood versus interstitial lactate concentrations

Analytes in ISF come from the blood through continuous capillaries[12] . Pores of their lining only allow small solutes, under approximately 70kDa, to pass across the capillary wall [221, 222]. Lactate molecular weight being 90 Da, it highly diffuses into the ISF and **Lactate ISF concentration ($[La^-]_{ISF}$) has a nearly 1:1 ratio correlation with $[La^-]_{cap}$** [95].

Dermal interstitial lactate concentrations

In healthy people, skin lactate concentration at rest is between 1 and 2.5 mmol/l [225]. **Resting dermal $[La^-]_{ISF}$ is in average about 30% higher than arterial $[La^-]_{pla}$** [225, 226]. Indeed, $[La^-]_{pla}$ at rest comprises between 0.5mmol/l and 2mmol/l in healthy humans, depending on people and time [227]. Like other tissues, the skin releases lactate. Skin contributes about 5% at rest to the whole-body lactate turnover [223]. However, despite the high proportion of whole-body lactate production by skin, **the evolution over time at rest of skin lactate concentration appear to reflect the evolution of the plasma concentration relatively well** [223]. The

Figure 3.14: Picture of the Lactate Pro 2, a commercially available blood lactate analyzer.

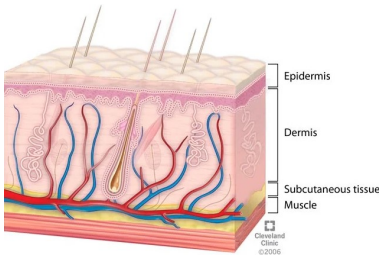

Figure 3.15: Schematic representation of the skin layers.

12: Depending on the location, continuous capillaries are generally the most present in the skin, and the least porous capillary type.

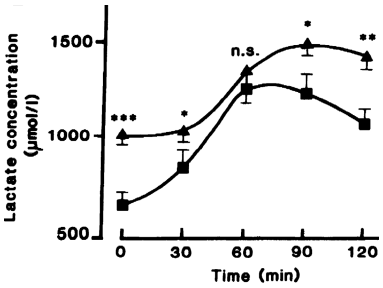

Figure 3.16: Evolution of $[La^-]_{pla}$ (square) and dermal $[La^-]_{ISF}$ (triangle) during an oral glucose tolerance test. From [223]

efficient blood-ISF bilateral diffusion of lactate seems to explain this correlation. As for glucose, lactate is subject to the inherent plasma-to-ISF lag [95]. An insufficient number of physiological studies address this delay for lactate. However, recent non-commercialized microneedle-based lactate biosensors suggest **a measured lag time of approximately 10 minutes relative to plasma variations** [228, 229]. The subcutaneous depth of the capillary plexus varies between 0.6 and 1.5 mm, depending on the on-body location [230]. Consequently, the delay between $[La^-]_{ISF}$ at the microneedles location and $[La^-]_{pla}$ may vary depending on the on-body location and Microneedles subcutaneous depth.

To our knowledge, **no study deals with the correlation between dermal $[La^-]_{ISF}$ and arterial $[La^-]_{pla}$ during exercise**. However, the net production of lactate by the muscles increases drastically during exercise compared to other organs, including the skin [178]. Consequently, the correlation between $[La^-]_{ISF}$ and $[La^-]_{pla}$ is probably better during exercise than at rest. Further studies remain necessary to quantify this correlation and possible parameters to be considered, such as the location on the body of the dermal ISF sampling and its proximity to the producing muscles. In addition, the dermal lactic concentration could vary depending on the depth under the skin. Krogstad et al. suggest a possible negative linear relationship between the catheter location in the dermal tissue layer and dermal $[La^-]_{ISF}$ during microdialysis measurements [231]. **Further studies are needed to confirm and quantify the influence of the microneedles depth of a minimally-invasive lactate monitoring device**.

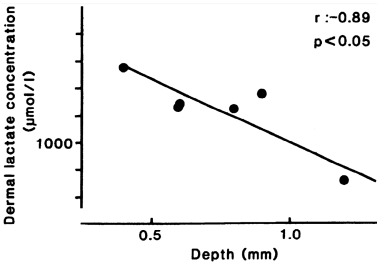

Figure 3.17: Measurement (n=6) of dermal concentration in either abdominal or forearm skin depends on the dermal tissue's catheter depth according to a linear relationship (R=-0.89, P < 0.05). From [223]

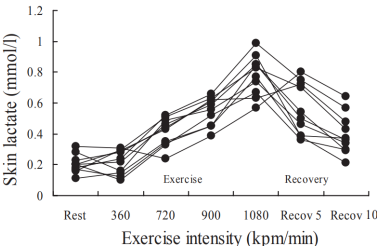

Figure 3.18: Lactate concentration of skin surface on working muscle at rest, during cycle exercise and recovery when one subject performed the same exercise ten times. From [224]

3.2.4 Conclusion

A report on the diffusivity status of lactate at rest and during activity is presented. During exercise, lactate is mainly released from muscle tissue. Synthesized by skeletal muscle cells, lactate diffuses throughout the body from the ISF of muscle cells to plasma, then from

capillary vessels to the subcutaneous and dermal ISF. Lactate's low molecular weight and high diffusivity suggest similar and correlated concentrations in extracellular fluid [95].

Few data are available on lactic acid concentrations in the skin and their variations during physical effort. Despite a consortium on the correlation between blood and interstitial concentrations, uncertainties in measurements of dermal ISF concentration remain greater than for glucose [232]. Depth in the dermis seems to have an impact on measured levels. Hydration may also be a factor in blood-tissue lactate crosstalk [232]. These parameters must be investigated to characterize the medical relevance of its monitoring in dermal ISF. **Further studies on lactate pharmacology are required to develop relevant, accurate, minimally-invasive lactate biosensors.**

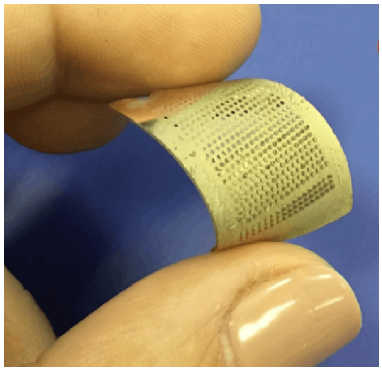

Figure 3.19: Flexible microneedles array developed by Caliò et al. From [233]

3.3 Fabrication of a Lactate Biosensor

3.3.1 Related Works

Several wearable microneedle-based enzymatic lactate biosensors have been developed.

Caliò et al. (2016) fabricated a lactate and glucose microneedles detection system [233]. They employed photolithography techniques to create polymer-based microneedles, incorporating the enzymes lactate oxidase (LOx) and glucose oxidase (GOx) into a photocurable mixture. Lactate and glucose are amperometrically detected in buffer-based solutions.

A notable feature of their approach is integrating enzyme and material in the same mixture, reducing the need for additional functionalization steps. Their proof-of-concept did not fully align with the clinically relevant concentration ranges for lactate (0.5–5 mM), highlighting the need for further optimization and calibration [233].

Bollella et al. (2019) developed a microneedle-based biosensor using a polycarbonate substrate with gold

Figure 3.20: Bollella et al.'s Polycarbonate structure of four 4x4 microneedle arrays metalized with gold and silver. From [234]

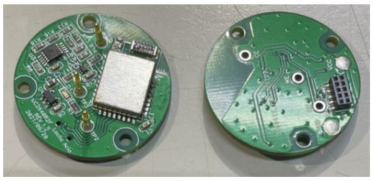

Figure 3.21: Front and back of the operational amplifier circuit of the wearable biosensor developed by Chien et al. From [229]

metallization on the working electrode [234, 235]. The working electrode was functionalized with electropolymerization with methylene blue and the enzyme chemical attachment via drop casting. This innovative device measures lactate concentration within a linear range of 0 to 100 μM in ISF and human blood serum. While these results fell short of measuring lactate within the clinically relevant range, they provided valuable insights into the impact of fluid complexity on sensor performance.

Figure 3.22: Sensors are installed on the leg's upper and lower parts during Chien *in vivo* experimentation. From [229]

Chien et al. (2022) developed a low-cost continuous lactate monitoring system (CLMS) based on a percutaneous microneedle array [229]. The working electrode has an area of 10 mm × 6 mm, including a 3 × 3 array of stainless-steel microneedles. Each needle's length, width, and thickness are 1 mm, 0.44 mm, and 0.03 mm, respectively. The working electrode is plated with gold, polyaniline, lactate enzyme, Nafion, and poly-HEMA. The reference electrode is a 2 × 1 array covered with silver chloride, and the counter electrode is a 2 × 1 array plated with gold. The sensor is incorporated into the CLMS and connected to a smartphone application and the cloud. The CLMS was tested on 40 human subjects who rode indoor bicycles, starting at 100 W and increasing in 25 W steps every 5 minutes until exhaustion. The wirelessly acquired data were analyzed to determine the subjects' lactate response to exercise [229].

The biosensor architecture developed in this thesis involves polypyrrole and lactate oxidase on a platinum substrate. The design of a miniature electronic system for signal acquisition is also covered.

3.3.2 Electronics

Potentiostat principles

A potentiostat is an electronic device used in electrochemistry to control the voltage between a working electrode and a reference electrode in an electrochemical cell [236]. This device and measuring tool allows to perform various electrochemical techniques, such

as cyclic voltammetry, linear sweep voltammetry, and amperometry [237]. Those techniques permit the study of the electrochemical properties of materials, monitoring chemical reactions, and investigating the behavior of electroactive species in solution. Potentiostats are employed for various purposes, including the study of corrosion mechanisms [238], the development of sensors and biosensors [239], and the investigation of electrocatalytic processes [240]. They can also be used in the fabrication of nanostructures [241], and for educational purposes in teaching electrochemistry fundamentals and applications [242].

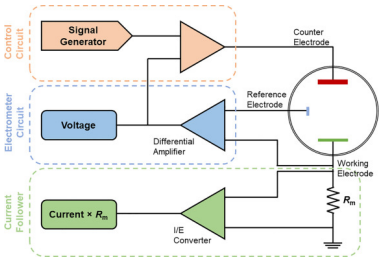

Figure 3.23: Simplified electronic diagram of a potentiostat. From [243]

A potentiostat maintains a constant potential difference between the working and reference electrodes while measuring the current that flows between the working and counter electrodes [237]. This allows researchers to study the relationship between the applied potential and the resulting current, providing valuable information about the electrochemical processes occurring at the electrode surface.

Figure 3.24: Commercial image of the PalmSens MultiEmstat3+ potentiostat. From [244]

LMP91000 characteristics

We opted for a cost-effective electronic development card: the LMP91000 of Texas Instruments [245]. The LMP91000 is an integrated analog front-end (AFE) chip manufactured by Texas Instruments (TI) and is specifically designed for use in electrochemical sensing applications. The card is comparable to high-end potentiostats costing several thousand euros. This board is not provided with data analysis software, like for commercialized potentiostats, such as the PSTrace package for PalmSens brand potentiostats [246]. In return for the affordable price, use involves programming in C++ and manually uploading the code for basic electrochemical experiments.

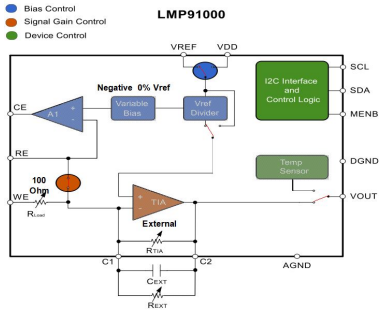

Figure 3.25: Electronic schematic of the Texas Instruments LMP91000 development board. Illustration taken from LMP91000 Sensor AFE Software [247].

The LMP91000 is designed for 3-lead single gas and 2-lead galvanic cell sensors. This device provides all the functionality for detecting changes in gas concentration based on a delta current at the working electrode. The LMP91000 generates an output voltage proportional to the cell current. The trans-impedance (TIA) gain is

program-controlled through an I2C-compatible interface by changing resistor values in the LMP91000. The TIA gain varies from 2.75 k to 350 k corresponding to a current range from 5 A to 750 A full scale. Optimized for micro-power applications, the LMP91000 AFE works over a 2.7 V to 5.25 V voltage range. The cell voltage is user-selectable using the onboard programmability. A temperature sensor is embedded and can be power cycled through the interface. The user reads the temperature sensor output through the VOUT pin. It is also possible to have both temperature output and output of the TIA simultaneously. Indeed, pin C2 is internally connected to the output of the trans-impedance (TIA), while the temperature is available at the VOUT pin. Depending on the configuration, the total current consumption for the device is less than 10 A. For power savings, the trans-impedance amplifier can be turned off and instead, a load impedance equivalent to the TIA's input impedance is switched in. [248]

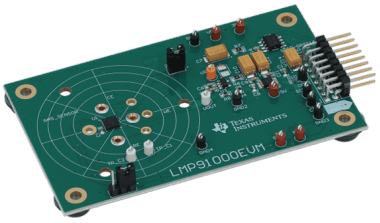

Figure 3.26: [247].

Key features of the LMP91000 include:

1. Sensor Interface: The chip can interface with various electrochemical sensors, including amperometric, potentiostatic, and galvanic cell sensors. It supports both three-electrode and two-electrode sensor configurations;
2. Programmable Gain: The LMP91000 allows the gain adjustment of the analog front-end to match the sensitivity of the connected sensor, making it suitable for a wide range of sensor types and applications;
3. Low Noise: It provides low noise and high precision, crucial for accurate measurements in electrochemical sensing applications;
4. Temperature Compensation: The chip includes features for temperature compensation, helping to maintain sensor accuracy even in varying temperature environments;
5. Integrated Voltage Reference: The board features an integrated voltage reference source, simplifying the design and calibration process;

6. Programmability: The AFE can be configured and programmed to meet the specific requirements of different sensors and applications, allowing for flexibility in sensor selection and calibration.

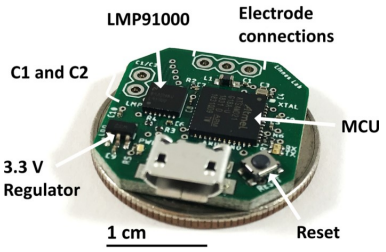

Figure 3.27: A coin-size potentiostat for wearable biosensors developed by Hoilett et al. [261].

The LMP91000 is involved in several research projects with biosensing applications, including: glucose [249, 250], sweat lactate [251, 252], urea detection [253, 254], viruses [255, 256], nucleic acid [257], estrogens [258], heavy metals in water [259] and other non-specific biomarker applications [260–263]

LMP91000 programming

Without modifications, the LMP91000 has an internal, 14-point bias circuit allowing for 14 different adjustable potentials between the working and reference electrodes. The LMP91000's internal bias circuitry sets the voltage reference and outputs a fraction of the voltage applied to LMP91000's VREF pin. The available biases are 0%, 1%, and from 2% to 22% in 2% steps. At an operating voltage of 3.3 V, a 14-point setting, provides a voltage resolution of about 66 mV and, at best, 54 mV voltage resolution at the LMP91000's lowest operating voltage of 2.7 V. We set up the LMP91000 as follows:

1. The Mode Control Register allows the configuration of the Operation Mode of the LMP91000. We set the MODECN variable to bit 0x03, which corresponds to the 3-lead amperometric cell mode;
2. TIA_GAIN parameter is defined at a 120 kΩ resistance. The load resistance is set to 100 Ω;
3. The Reference control register (REFCN) allows the configuration of the Internal zero, the Bias, and the Reference source. We set the Bias on the eleventh bit, which corresponds to 24% of the reference electrode potential. The voltage source is defined as internal and positive.

The reference voltage applied to the LMP91000 is 2.5 Volts. The standard electrode potential of hydrogen peroxide oxidation is 0.68 V. By setting the cell bias voltage at 24% of the reference voltage, the maximum value allowed, we obtain a bias voltage of 0.6V. Therefore,

the potential applied at the CE is slightly lower than the H_2O_2 standard electrode potential. As a result, the oxidation reaction can be slowed down.

A WeMos D1 Mini controls the LMP91000. The Linnes-Lab code available on Github was used to carry out chronoamperometry[13] [266]. The easy exploitation of the data measured by chronoamperometry justifies this technical choice.

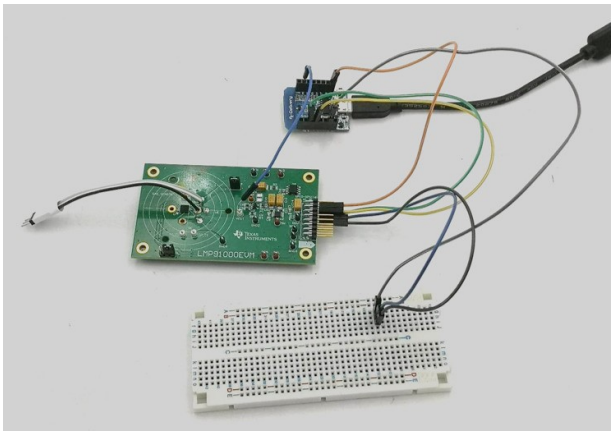

Figure 3.29: The WeMos D1 mini controlling the LMP91000.

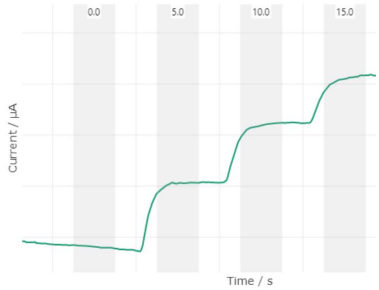

Figure 3.28: Example of chronoamperometry with a 5 mM concentration steps, from 0 to 15 mM. The current intensity is measured at regular intervals. Sensor sensitivity is calculated by dividing the current variation by the concentration variation over a given concentration range. From [103]

13: Chronoamperometry is a time-dependent technique applying a potential to the WE in an electrochemical cell, allowing for the electrolysis of a chemical species while measuring the current. The current between the WE and RE is linearly correlated to the analyte concentration toward the sensor surface. [264, 265]

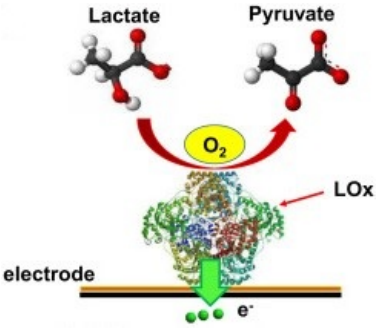

Figure 3.30: Lactate oxidation into pyruvate, catalyzed by LOx. Dioxygen must be abundant. From [267]

3.3.3 Chemical Functionalization

A rigorous protocol was defined and followed to perform the functionalization of the lactate biosensor on a platinum wire. The equipment used is as follows: LMP91000 from Texas Instrument and a WeMos D1 mini, Lactate Oxidase (LOx), PolyPyrrol (PPy), piece of pure platinum wire, lactic acid solution, Phosphate Buffer Saline (PBS), Soda, magnetic stirrer, a 1ml electronic micropipette, a 2ml Eppendorf tube, a 500 ml beaker, crocodile clips.

Chemical cleaning of platinum wires

Functionalization tests were carried out on a metal wire before resorting to microneedles. The wire used is 99.99% platinum, with a diameter of 0.3 millimeters, sold by Vrttlkkfe [268]. Platinum is often used in biosensors due to its high catalytic activity, high electrical conductivity, and biocompatibility [269]. Other metals used in biosensors are gold, palladium, rhodium, ruthenium and copper [270].

We sanded the wire to remove any surface treatment and cut several pieces of approximately 5 centimeters in length. These pieces have undergone chemical cleaning. 0.8g of solid soda was dissolved in a 100 ml beaker of distilled water. The wires were immersed in the soda solution for 10 minutes, before being cleaned thoroughly with ethanol, and dried at room temperature. Chemical cleaning removes contaminants or impurities from the platinum surface.

PPy solution preparation

PPY is one of the most extensively used conducting polymers to design bioanalytical sensors[271]. We prepared a polypyrrole solution by dissolving 0.4 g of PPy powder in 20 mL of acetone. The mixture was stirred for 30 minutes at room temperature until the PPy powder was fully dissolved. 80 ml of distilled water was added to the solution and stirred for 15 minutes to obtain a homogeneous PPy solution.

Immobilization matrix dip-coating

The platinum wire intended for the WE was dip-coated with PPy. Immobilization matrix dip coating is used to immobilize or attach biomolecules, such as enzymes or antibodies, onto a surface. This process involves immersing or dipping, a substrate into a coating material solution [272, 273]. We dipped the cleaned platinum wire into the PPy solution and withdrew it slowly at approximately 2 cm/min for 2 minutes. The coated wire was then dried at 60°C in an oven for 30 minutes.

Preparation of the functionalization solution

Functionalization solution is a solution used to modify the surface of a material to enhance its properties for a specific application [274]. In the context of enzymatic biosensors, a functionalization solution is used to modify the biosensor's surface to enhance the enzyme's immobilization and improve its stability and activity. Lactate oxidase is an enzyme produced by various microorganisms [275]. LOx catalyzes lactate oxidation to pyruvate and hydrogen peroxide [276]. We pour 2 µl of LOx in a

2 ml Eppendorf tube using a micropipette and 2 ml of PBS, shaking the tube vigorously to homogenize.

Enzyme immobilization

Biosensor functionalization consists of immobilizing the enzyme on a transducer surface [277]. The four main immobilization methods are (1) non-covalent adsorption and deposition, (2) physical entrapment, (3) covalent attachment, and (4) bio-conjugation (figure 3.32). LOx is immobilized by physical entrapment [278]. Physical entrapment consists of the enzymes' inclusion in a polymer matrix. Enzymes' physical entrapment in PPy has been reported to enhance the stability and activity of the enzyme [279].

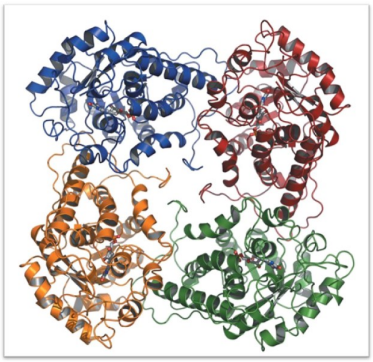

Figure 3.31: Molecular 3D representation of the lactate oxidase.

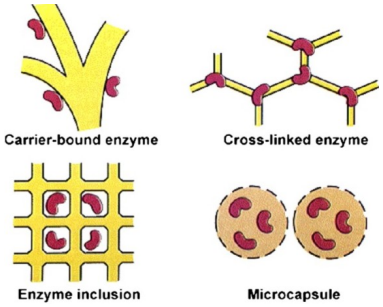

Figure 3.32: Main methods used for enzyme immobilization. From [278].

0.2ml of the functionalization solution was drop cast onto the last 2 cm platinum wire to immerse the PPy-coated platinum wire. The wire was left immersed for 12 hours at room temperature. The PPy 3D structure should entrap the enzyme molecules. The wire was removed from the lactate oxidase solution and washed with PBS.

The experiment to characterize the designed biosensor is presented in the Experimentation section.

3.3.4 Microneedles Fabrication

Microneedles design

Once the proof of concept of the biosensor has been car-

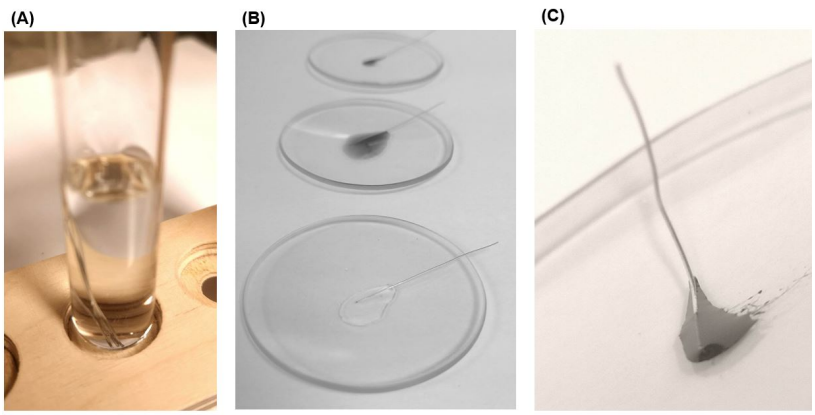

Figure 3.33: (A) Chemical cleaning with a soda solution (0.2mM). (B) Stationary PPy deposition tests. Activated carbon powder was used to try and increase conductivity. (C) Drop-casting the functionalization solution.

ried out on microneedles, the challenge is to reproduce the experiment on microneedles. A microneedle module for the BioWatch has been modeled in 3D. The first version is a ring, with a diameter of 2.5 centimeters. It has 12 microneedles of 0.8 millimeters in height. The placement of the needles was set to be connected by tracks. The tracks are hand-painted with conductive paste. The WE and CE tracks each connect four microneedles. Four additional needles are also provided for the RE in another version for three-electrode mode. The final version has 18 microneedles - 6 for each electrode - spaced 4 millimeters apart.

BioWatch integration system

Three slots are provided for the integration of Pogo pin connectors. Spring-loaded pins ensure the connection of the painted track on the microneedles with the female pins of the BioWatch potentiostat PCB. The WE, CE, and RE tracks are thus connected to the associated electronic leads for signal acquisition. An equilateral triangle encompasses the ring in the microneedles module's final version. Three magnets of two millimeters in diameter fit at each corner. The combination of connectors and magnets ensures the pluggable and changeable nature of the microneedle module. This system makes a real contribution to BioWatch, by only disposing of the microneedle module at the end of the life of the biosensor. The current design of marketed CGMs often involves throwing away the entire electronic system.

Microneedles 3D printing

The module is 3D printed. The printer used is a Form 3+ from Formlabs. Form 3+ is a desktop Stereolithography 3D printer powered by Low Force Stereolithography (LFS) technology and engineered to obtain exceptional print quality with hassle-free post-processing [280]. The material used is BioMed Clear Resin V4 from Formlabs [281]. The rigid and transparent resin is suitable for biocompatible applications requiring long-term skin or mucosal membrane contact.

Laser printing was carried out with a layer thickness

of 25µm. The post-treatment process consists of rinsing with ethanol and drying in the oven at 40°C for 20 minutes. This temperature, lower than the recommended 60°C [282], limits material contraction and preserves the sharp shape of the Microneedles. After the post-treatment, the pogo pins and the magnets are integrated by simple embedding.

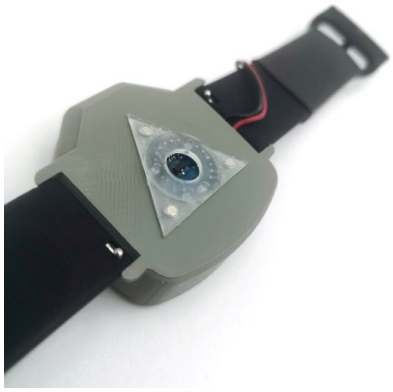

Figure 3.34: The microneedles module disposed under the BioWatch. Three magnets secure the module in place.

Metallization of microneedles

The metallization was done with platinum paste PT1 from Greatcell Sollar Materials [283]. The paste was applied to the needles. The tracks could be roughly traced using a micropipette and a toothpick. The microneedle module is then dried in the oven at 200°C for half an hour. Drying allows uniformly distributed platinum nanoclusters, providing transparency and high catalytic activity. However, the platinum paste turned out to be too viscous. Before the paste could dry, the volume deposited expanded widely, mixing the different tracks. Once dry, the measured conductivity is almost zero. Too low a drying temperature can also explain this.

3.3.5 Evaluation

The platinum wire biosensor was tested in vitro. An experimental setup was carried out under measured laboratory conditions.

Set-up

The LMP91000 board is set in 3-electrode chronoamperometry mode. The WeMos drives the AFE. Two

pre-cleaned platinum wires are connected to the RE and CE leads. A third wire, functionalized according to the above protocol, is connected similarly to the WE. A beaker was filled with 400 ml of PBS. The three wires are positioned to be immersed by about two centimeters, without touching the walls.

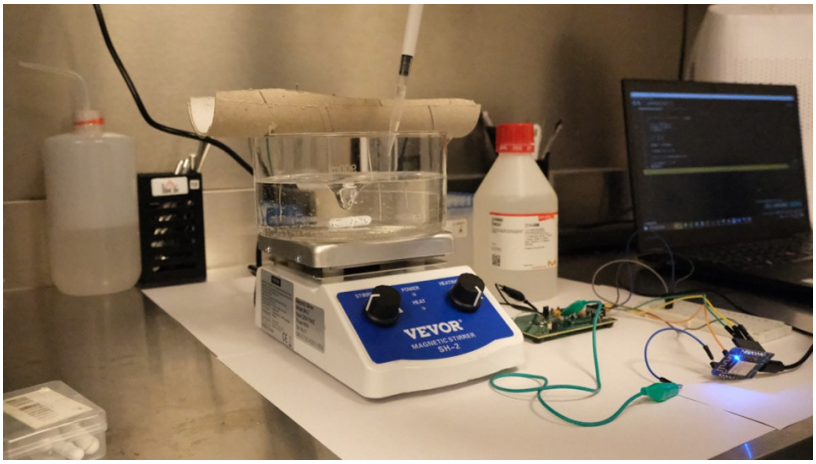

Figure 3.35: Experimental set-up. A carton support maintains the three wires/electrodes immersed and immobile.

Protocol

The Arduino program is run. After 45 minutes, the current offset is relatively stable. The first dose of 1.5ml lactic acid is injected into the beaker using an electronic micro-pipette. This dose corresponds to a concentration of XX mol/ml. Three minutes later, another 1.5ml of lactic acid is added. The operation is repeated 10 times.

$$C_3H_6O_3 + O_2 \leftrightharpoons C_3H_4O_3 + H_2O_2 \quad (3.1)$$
$$H_2O_2 \leftrightharpoons O_2 + 2H^+ + 2e^- \quad (3.2)$$

Figure 3.36: (3.3) Lactate oxidation to pyruvate and hydrogen peroxide and (3.4) hydrogen peroxide oxidation.

Throughout the experiment, current intensity is measured every second. After the tenth injection, chronoamperometry is stopped. Data are exported in CSV format. The CSV file generated is imported into PalmSense's PSTrace 5.9 software [284]. The software enables temporal visualization of the evolution of the current measured during chronoamperometry. The sensor can be considered functional if significant increases in current intensity coincide with lactic acid injection timing.

A total of seven sensors were tested under different

conditions. Only one experiment proved conclusive, with current plateauing at certain injections. This low success rate is probably due to electronic connection problems. The functional sensor was characterized. Its sensitivity is 1.8 nA/mM. Its detection limit is less than 5 mM and its detection range extends from 5 to 20 mM.

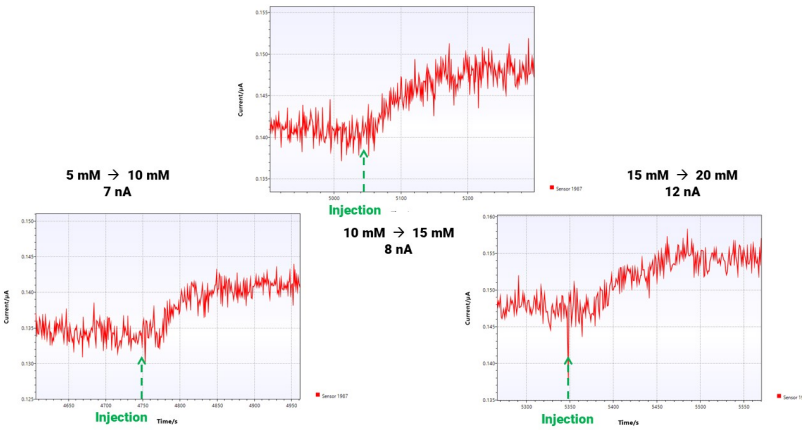

Figure 3.37: Zoom in on the stages corresponding to lactic acid injection on the chronoamperometric curve.

3.3.6 Future works

Chemistry

The biosensor developed has some technical limitations. The calculated sensitivity is relatively low compared with the state of the art. Similar lactate biosensors have a sensitivity about ten times higher. One potential explanation is the poor immobilization of LOx on the platinum surface. Sensor stability and reproducibility also remain to be quantified. At the chemical level, future surface analysis work would enable assessing the enzyme immobilization quality. Cyclic voltammetry in a Fe^{2+}/Fe^{3+} solution would optimize the cleaning and deposition steps. Other deposition techniques can improve sensor performance, such as electrodeposition. Immobilization by adsorption rather than simple entrapment in the polymer matrix would increase the biosensor's lifetime, which remains to be determined through long-term testing.

Electronics

In terms of electronics, the signal acquisition setup needs significant improvement. The current setup favors wire connection errors, and hence debugging time and data loss during chronoamperometry. Testing with a commercial potentiostat could alleviate this problem, facilitating biosensor optimization through advanced electrochemical analysis.

Microneedles transposition

The miniaturization of the wires-based biosensor into a microneedle biosensor also remains unachieved. A technical solution for needle metallization should enable tracing distinct tracks. The metallization process requires heating the microneedle module sufficiently to dry the paste and ensure the platinum particles monodispersion, without melting the resin. Experimentation with other, less viscous platinum pastes, with drying temperatures below the resin oxidation temperature of 250°C [285], is necessary. Nanochemazone's platinum paste with a drying temperature of 150°C and a modifiable viscosity should be considered for these future tests [286].

BioWatch integration

Finally, work on integrating the microneedle module into the BioWatch must be pursued. The miniature electronic board for signal acquisition and processing is designed but not printed. Pogo pin connectors must be adapted to this new board. Once functional, this board can be merged with the BioWatch operating board through advanced electronic engineering.

3.3.7 Conclusion

This study detailed the development of a microneedle-based lactate biosensor, encompassing the various stages from conception to evaluation. A proof of concept for a lactate biosensor on platinum wire has been developed. The microneedle module provides BioWatch with minimally-invasive biomarker monitoring functionality. While challenges were encountered in microneedle biosensor fabrication, the groundwork laid demonstrates

promising potential for wearable biosensing technology. This study provides valuable insights into wearable biosensors and establishes a foundation for future research and development.

3.4 Interactive 3D Modeling Of The Molecular-Scale Microneedle Biosensor

An educational application, called Bione, has been developed to image the microneedle biosensor working *in vivo*. Lactate oxidase (LOx) is replaced by glucose oxidase (GOx), changing the lactate sensor into a glucose sensor. As glucose monitoring is better known than lactate monitoring, this change makes Bione more accessible to a wider audience, with greater public involvement. Besides the enzyme, the chemical architecture of glucose and lactate sensors is identical. This complementary work aims to popularize the physical and chemical principles involved in biosensors. The application is open-source, developed and accessible on the Cables.gl platform [287].

Cables.gl is a WebGL-based tool for building and compositing real-time interactive animations [288]. The particularity of this tool is to allow rapid assembly of prebuilt blocks of complex JavaScript code, called "operators". Cables.gl programming works by linking operators to construct a scene. Different operators let users manipulate textures, 3D meshes and data structures such as Objects, Arrays and file formats such as JSON. The parameters of the previous operators are propagated along the tree structure [289].

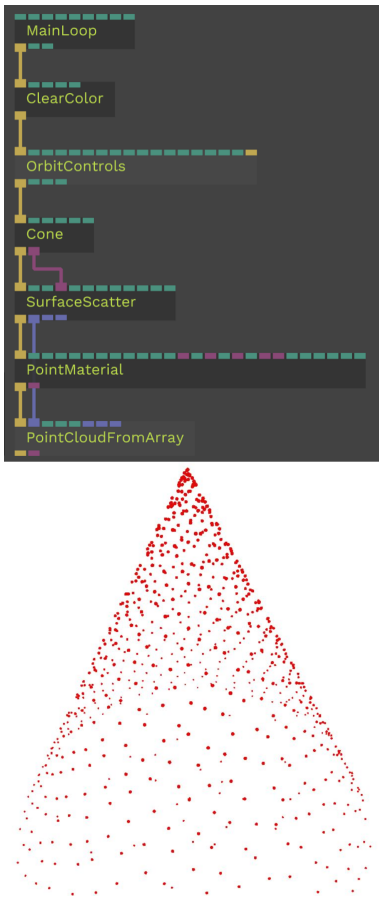

Figure 3.38: Example of operator assembly on Cables.gl to generate a set of random points on a cone surface with 3D navigation.

3.4.1 Architecture overview

Bione is constituted of 3D mesh elements. The three microneedles and their support were modelized on SolidWorks, as well as a human cell in a simplified

cobblestone shape. A 3D array is modeled with one cell in each location. An animation of exaggerated and randomized contraction and cell expansion gives the skin a living appearance. The microneedle holder is placed on the skin surface. The microneedles pierce the skin. The tip protrudes beyond the modeled skin layer for better visualization. A pitching movement of the camera brings realism and immersion.

The user can navigate through three camera views. The first allows to visualize the complete scene. The learner can observe the glucose molecule flux from the ISF in contact with the WE microneedle, and the current generated and measured. The second is a zoom on the WE microneedle. This view includes the electrons released from the hydrogen peroxide oxidations and their movement to the CE. The third camera zooms in on the WE microneedle surface. The user can visualize the different chemical layers on the metalized needle.

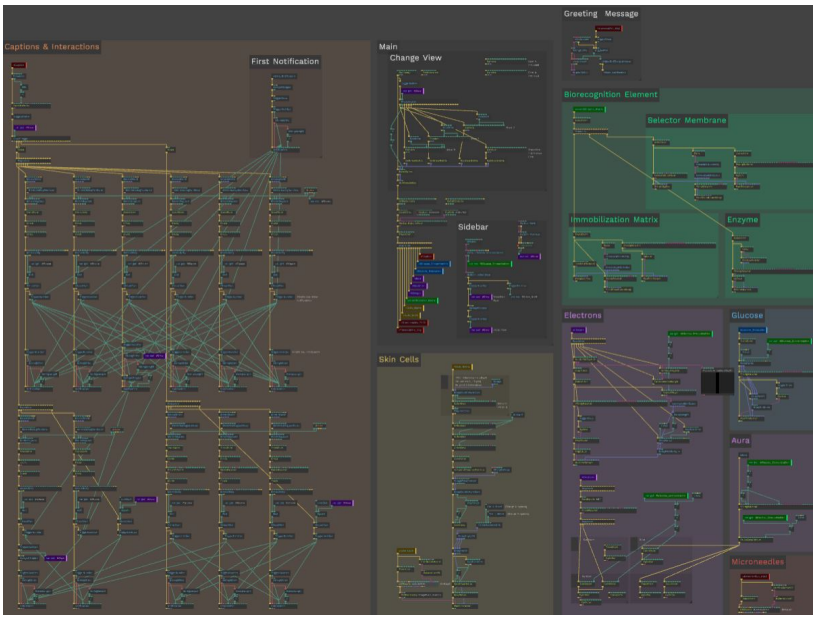

Figure 3.39: Architecture of the no-code open-source application.

Transitions allow to switch smoothly from one view to another. In each view, a sidebar controls the analyte concentration value, in this case, glucose. The variation of modeled glucose molecules is thus proportional to the variation in the blood sugar level adjusted by the user. The behavior of the generated electrons and current is also lively changed.

A trigger network displays explanations to the user. Clicking on the highlighted round indicators causes the appearance of an explanatory text on the element in question. The captions are written with a simple vocabulary to be understandable by an uninformed public. The following elements are thus dealt with: the WE, the CE, the RE, the ISF, the electrons generated by oxidation and the resulting current, the immobilization matrix, the enzyme, and the selective membrane.

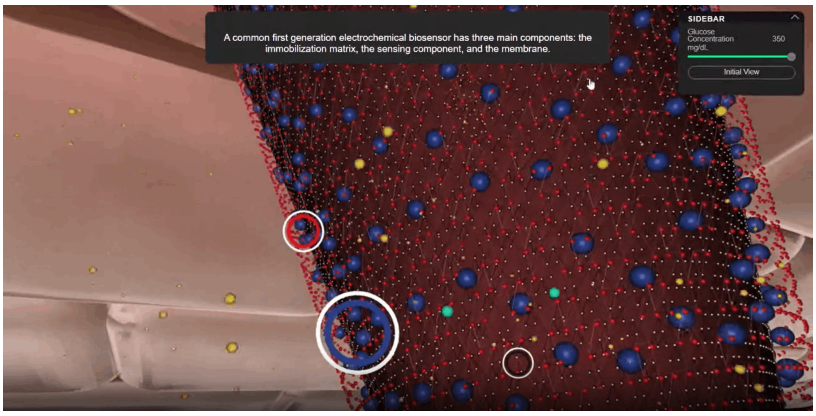

Figure 3.40: Screenshot of the Bione application.

3.4.2 Evaluation

The application was tested by 10 undergraduate students uninitiated in electrochemistry. Students could navigate and interact with Bione from their home computer for 15 minutes. The ten students report that Bione is intuitive and easy to use. All of them understood the concepts discussed and could explain them again. Eight of them said they were impressed by the graphics. Nine subjects felt immersed.

3.4.3 Future works

Future works should optimize Bione's performance. Certain graphics cards poorly support the current application. This optimization will also enable Bione to be integrated into a dedicated educational web platform. Supporting other biomarkers would raise users' awareness of possible medical applications for wearable biosensors.

3.4.4 Conclusion

Bione is the first interactive 3D application to learn the basic principles of biosensors. The web app bridges the gap between basic pharmacology and electrochemistry to illustrate the challenges of wearable biosensor design. The representation of a microneedle-based biosensor in human skin can be used to inform potential future wearers. The application popularizes the functioning of the lactate microneedle biosensor developed for the BioWatch. Finally, Bione makes the science of biosensors more accessible.

3.5 Conclusion

Wearable lactate biosensors have the potential to revolutionize the field of sports physiology by providing real-time, non-invasive monitoring of lactate levels during exercise. Recent advances in materials science, microfabrication, and wireless communication technologies have driven the development of these biosensors.

This chapter deals with lactate pharmacology during exercise, to better understand the biological issues involved in monitoring this analyte in the ISF. The literature review comprehensively explains lactic acid concentrations in dermal ISF by addressing the challenges micro-needle lactate sensor developers face.

The development of a lactate sensor includes programming a physicochemical signal acquisition and processing board, designing the biosensor's chemical architecture and a microneedle module for the sensor's wearability. In vitro tests demonstrate and characterize the sensor performances. The transposition of the biosensor to an innovative microneedle configuration has been initiated. The module presented is a 3D resin print. The skin penetration capability of the microneedles is painless and satisfactory for performing measurements in dermal ISF. A method of metalizing the needles with a platinum paste proved inconclusive.

The design of the first interactive 3D application for learning about biosensors is covered. The digital platform helps to promote this discipline. The innovative WebGL solution demonstrates promising pedagogical performance for teaching physicochemical principles.

The work presented in this chapter contributes to researching and popularizing microneedle biosensors for minimally-invasive biomarker monitoring with smartwatches. Integrating ISF biomonitoring into smartwatches could drastically improve the health and experience of athletes and patients.

4 Conclusion

Work presented in this thesis leads to significant advances in designing high-performance, non-invasive wearable biosensor systems with optimized user experience. The potential of integrating biosensors with smartwatches for user experience and multi-analyte monitoring has been demonstrated by developing a smartwatch prototype and wearable biosensors. An autonomous microfluidic system for monitoring glucose in sweat has been assembled, and the full development of a micro-needle lactate biosensor has been initiated. These two biosensors meet the monitoring needs of diabetic and sports medicine. Their respective wireless and embedded connections with the BioWatch **demonstrate the potential of smartwatches as a modular platform for implementing wearable biosensors**.

Over and above the state-of-the-art knowledge on lactate behavior in the body, this thesis promotes a biosensor design strategy intrinsically based on biomarker pharmacology. **The triptych of technical performance, user experience, and medical relevance should thus drive the development of biomonitoring systems**. The smartwatch is likely to be the wearable of the future, discreetly integrating non-invasive biosensors to monitor our health and well-being. The development of educational applications such as Bione would facilitate this advent by popularizing the basic physicochemical principles involved in biosensors. **Empowering smartwatches with molecular detection technology would elevate these intelligent accessories into veritable personal medical coaches, assisting healthcare professionals with comprehensive medical data.**

Acknowledgements

Merci à Gregor Jouet, Gaétan Carrade et Dimitry Siebert pour leur contribution.

Merci à l'équipe enseignante du DVIC pour m'avoir initié au monde de la tech et de la recherche : Madalina Nicolae, Brice Parilusysan, Yliess Hati, Zacharie Guillaume, Paul-Peter Arslan, Xiao Xiao, Marc Teyssier et Clément Duhart.

Merci à Fabien Caura, Jonah Marrs et Pierrick Chevron pour leurs enseignements en électronique. Merci également à Marie Julou, Thomas Juldo et Nicolas Stass pour leur aide.

Merci beaucoup à Youssef Lattach et Syrine Chebil pour m'avoir initié à l'électrochimie appliquée aux biocapteurs.

Un grand merci à l'équipe PKvitality pour m'avoir formé et embarqué au plus près de la conception de la K'Watch : Lucas Giralt, Sehar Abbas, Arnaud Malet et toute l'équipe.

Merci à l'équipe de R4Innov avec qui j'ai amélioré mon écriture et pu aider de belles entreprises françaises à se développer : Jérémy Ohayon, Benjamin Haas, Jérôme Halary et les autres.

Merci à mes camarades de classe et amis pour leur solidarité, leur détermination stimulante et nos bons moments partagés : Romain Manoïlov, Louis-Maris Restout, Wim Poignon, Tristan Journel, Philibert Le Gonidec de Kerhalic, Maxime Broussart, Louis Badr, Jérémie Leibl, Adrien Lefevre et Hugo Dardill. Merci à Adem Rahal sans qui ces rencontres n'auraient pas été possibles.

References

[1] Luigi Atzori, Antonio Iera, and Giacomo Morabito. 'The Internet of Things: A survey'. In: *Computer Networks* 54.15 (Oct. 28, 2010), pp. 2787–2805. DOI: 10.1016/j.comnet.2010.05.010. (Visited on 07/02/2023) (cited on page 4).

[2] Hongki Cha, Wonsuk Lee, and Jonghong Jeon. 'Standardization strategy for the Internet of wearable things'. In: *2015 International Conference on Information and Communication Technology Convergence (ICTC)*. Oct. 2015, pp. 1138–1142. DOI: 10.1109/ICTC.2015.7354758 (cited on page 4).

[3] Suranga Seneviratne et al. 'A Survey of Wearable Devices and Challenges'. In: *IEEE Communications Surveys & Tutorials* 19.4 (2017), pp. 2573–2620. DOI: 10.1109/COMST.2017.2731979 (cited on page 4).

[4] Aleksandr Ometov et al. 'A Survey on Wearable Technology: History, State-of-the-Art and Current Challenges'. In: *Computer Networks* (Apr. 1, 2021), p. 108074. DOI: 10.1016/j.comnet.2021.108074 (cited on pages 4, 6, 15).

[5] Edward O. Thorp. *Beat the dealer: A winning strategy for the game of twenty-one*. Vol. 310. Vintage, 1966 (cited on page 4).

[6] T Poongodi et al. 'Wearable devices and IoT'. In: *A handbook of Internet of Things in biomedical and cyber physical system* (2020), pp. 245–273 (cited on page 4).

[7] Rajendra Singh Bisht, Sourabh Jain, and Naveen Tewari. 'Study of wearable IoT devices in 2021: Analysis & future prospects'. In: (2021), pp. 577–581 (cited on page 4).

[8] Aodhán Hickey. *The rise of wearables: From innovation to implementation*. 2021 (cited on page 4).

[9] F John Dian, Reza Vahidnia, and Alireza Rahmati. 'Wearables and the Internet of Things (IoT), applications, opportunities, and challenges: A Survey'. In: *IEEE access* 8 (2020), pp. 69200–69211 (cited on pages 4, 5).

[10] Robin Singh Chandel et al. 'Smart watches: A review of evolution in bio-medical sector'. In: *Materials Today: Proceedings* 50 (2022), pp. 1053–1066 (cited on page 4).

[11] Tracey te Braake. *Smartwatches: Transforming Daily Life*. Medium. June 29, 2023. URL: https://medium.com/@tebraaketracey/smartwatches-transforming-daily-life-604f334e50e1 (visited on 08/25/2023) (cited on page 4).

[12] Daoyan Jin et al. 'Self-tracking behaviour in physical activity: a systematic review of drivers and outcomes of fitness tracking'. In: *Behaviour & Information Technology* 41.2 (Jan. 25, 2022), pp. 242–261. DOI: 10.1080/0144929X.2020.1801840. (Visited on 08/25/2023) (cited on page 5).

[13] Dawon Kim and Yosoon Choi. 'Applications of Smart Glasses in Applied Sciences: A Systematic Review'. In: *Applied Sciences* 11.11 (Jan. 2021), p. 4956. DOI: 10.3390/app11114956. (Visited on 08/25/2023) (cited on page 5).

[14] Rebecca R. Ruckdashel, Ninad Khadse, and Jay Hoon Park. 'Smart E-Textiles: Overview of Components and Outlook'. In: *Sensors* 22.16 (Jan. 2022), p. 6055. DOI: 10.3390/s22166055. (Visited on 08/25/2023) (cited on page 5).

[15] Aleksandr Ometov et al. 'A survey on wearable technology: History, state-of-the-art and current challenges'. In: *Computer Networks* 193 (2021), p. 108074 (cited on page 5).

[16] Lin Lu et al. 'Wearable health devices in health care: narrative systematic review'. In: *JMIR mHealth and uHealth* 8.11 (2020), e18907 (cited on page 5).

[17] Vishal Patel et al. 'Trends in workplace wearable technologies and connected-worker solutions for next-generation occupational safety, health, and productivity'. In: *Advanced Intelligent Systems* 4.1 (2022), p. 2100099 (cited on pages 5, 6).

[18] Research and Markets. *Global Smart Wearable Entertainment Devices and Services Market 2016-2020*. Aug. 2016. URL: https://www.prnewswire.com/news-releases/research-and-markets---global-smart-wearable-entertainment-devices-and-services-market-2016-2020-with-att-ee-sprint--telefonica-dominating-300322497.html (cited on page 5).

[19] Serhat Burmaoglu et al. 'Chapter 14 - Evolution Map of Wearable Technology Patents for Healthcare Field'. In: *Wearable Technology in Medicine and Health Care*. Ed. by Raymond Kai-Yu Tong. Academic Press, 2018, pp. 275–290. DOI: https://doi.org/10.1016/B978-0-12-811810-8.00014-2 (cited on page 5).

[20] NPD Group. *Smartwatch Functions People Use the Most*. Accessed on September 23, 2023. Aug. 2017 (cited on page 5).

[21] Jonathan M Peake, Graham Kerr, and John P Sullivan. 'A critical review of consumer wearables, mobile applications, and equipment for providing biofeedback, monitoring stress, and sleep in physically active populations'. In: *Frontiers in physiology* 9 (2018), p. 743 (cited on page 6).

[22] Matthew Smuck et al. 'The emerging clinical role of wearables: factors for successful implementation in healthcare'. In: *NPJ Digit Med* 4 (Mar. 10, 2021), p. 45. DOI: 10.1038/s41746-021-00418-3. (Visited on 07/15/2023) (cited on pages 6, 7).

[23] Geoff Appelboom et al. 'Smart wearable body sensors for patient self-assessment and monitoring'. In: *Archives of Public Health* 72.1 (), p. 28. DOI: 10.1186/2049-3258-72-28 (cited on page 6).

[24] Sumit Majumder, Tapas Mondal, and M. Jamal Deen. 'Wearable Sensors for Remote Health Monitoring'. In: *Sensors* 17.1 (Jan. 2017), p. 130. DOI: 10.3390/s17010130. (Visited on 08/25/2023) (cited on page 6).

[25] Farida Sabry et al. 'Machine Learning for Healthcare Wearable Devices: The Big Picture'. In: *Journal of Healthcare Engineering* 2022 (Apr. 18, 2022), e4653923. DOI: 10.1155/2022/4653923. (Visited on 08/25/2023) (cited on page 6).

[26] Mitesh S. Patel, David A. Asch, and Kevin G. Volpp. 'Wearable Devices as Facilitators, Not Drivers, of Health Behavior Change'. In: *JAMA* 313.5 (Feb. 3, 2015), pp. 459–460. DOI: 10.1001/jama.2014.14781. (Visited on 08/25/2023) (cited on page 6).

[27] Harjeevan Singh Kang and Mark Exworthy. 'Wearing the Future—Wearables to Empower Users to Take Greater Responsibility for Their Health and Care: Scoping Review'. In: *JMIR Mhealth Uhealth* 10.7 (July 13, 2022), e35684. DOI: 10.2196/35684 (cited on page 6).

[28] Lukasz Piwek et al. 'The Rise of Consumer Health Wearables: Promises and Barriers'. In: *PLoS Med* 13.2 (Feb. 2016), e1001953. DOI: 10.1371/journal.pmed.1001953 (cited on page 6).

[29] Bill Fera. *Improving care and creating efficiencies*. Deloitte Insights. Sept. 2020. URL: https://www2.deloitte.com/us/en/insights/industry/health-care/digital-health-trends.html (visited on 07/16/2023) (cited on page 6).

[30] Joel M Raja et al. 'Apple watch, wearables, and heart rhythm: where do we stand?' In: *Annals of translational medicine* 7.17 (2019) (cited on page 6).

[31] Stefano Canali, Viola Schiaffonati, and Andrea Aliverti. 'Challenges and recommendations for wearable devices in digital health: Data quality, interoperability, health equity, fairness'. In: *PLOS Digit Health* 1.10 (Oct. 13, 2022), e0000104. DOI: 10.1371/journal.pdig.0000104 (cited on page 6).

[32] Nancy F. Butte, Ulf Ekelund, and Klaas R. Westerterp. 'Assessing physical activity using wearable monitors: measures of physical activity'. In: *Med Sci Sports Exerc* 44.1 (Jan. 2012), S5–12. DOI: 10.1249/MSS.0b013e3182399c0e (cited on page 6).

[33] Jennifer A. Schrack et al. 'Assessing Daily Physical Activity in Older Adults: Unraveling the Complexity of Monitors, Measures, and Methods'. In: *J Gerontol A Biol Sci Med Sci* 71.8 (Aug. 2016), pp. 1039–1048. DOI: 10.1093/gerona/glw026 (cited on page 6).

[34] Connor D Flynn et al. 'Biomolecular sensors for advanced physiological monitoring'. In: *Nature Reviews Bioengineering* (2023), pp. 1–16 (cited on pages 7, 8).

[35] Priti Singh et al. 'Biomedical perspective of electrochemical nanobiosensor'. In: *Nano-micro letters* 8 (2016), pp. 193–203 (cited on page 7).

[36] Atul Sharma et al. 'Wearable biosensors: an alternative and practical approach in healthcare and disease monitoring'. In: *Molecules* 26.3 (2021), p. 748 (cited on pages 7, 8).

[37] Guanglei Li and Dan Wen. 'Wearable biochemical sensors for human health monitoring: sensing materials and manufacturing technologies'. In: *Journal of materials chemistry B* 8.16 (2020), pp. 3423–3436 (cited on page 7).

[38] A. P. Turner. 'Tech.Sight. Biochemistry. Biosensors–sense and sensitivity'. In: *Science* 290.5495 (Nov. 17, 2000), pp. 1315–1317. DOI: 10.1126/science.290.5495.1315 (cited on page 7).

[39] Abid Haleem et al. 'Biosensors applications in medical field: A brief review'. In: *Sensors International* 2 (Jan. 1, 2021), p. 100100. DOI: 10.1016/j.sintl.2021.100100. (Visited on 07/15/2023) (cited on page 7).

[40] Varnakavi Naresh and Nohyun Lee. 'A Review on Biosensors and Recent Development of Nanostructured Materials-Enabled Biosensors'. In: *Sensors* 21.4 (Jan. 2021), p. 1109. DOI: 10.3390/s21041109. (Visited on 07/15/2023) (cited on page 7).

[41] Yiran Yang and Wei Gao. 'Wearable and flexible electronics for continuous molecular monitoring'. In: *Chem Soc Rev* 48.6 (Mar. 18, 2019), pp. 1465–1491. DOI: 10.1039/c7cs00730b (cited on pages 7, 9).

[42] Kyeonghye Guk et al. 'Evolution of wearable devices with real-time disease monitoring for personalized healthcare'. In: *Nanomaterials* 9.6 (2019), p. 813 (cited on page 7).

[43] Kateryna Shavanova et al. 'Application of 2D non-graphene materials and 2D oxide nanostructures for biosensing technology'. In: *Sensors* 16.2 (2016), p. 223 (cited on pages 7, 8).

[44] Jayoung Kim. 'Wearable Electrochemical Biosensors for Healthcare Monitoring Applications'. In: 2018. (Visited on 07/15/2023) (cited on page 7).

[45] L. C. Clark and C. Lyons. 'Electrode systems for continuous monitoring in cardiovascular surgery'. In: *Ann N Y Acad Sci* 102 (Oct. 31, 1962), pp. 29–45. DOI: 10.1111/j.1749-6632.1962.tb13623.x (cited on page 7).

[46] S. J. Updike and G. P. Hicks. 'Reagentless substrate analysis with immobilized enzymes'. In: *Science* 158.3798 (Oct. 13, 1967), pp. 270–272. DOI: 10.1126/science.158.3798.270 (cited on page 7).

[47] C. Diviés. 'Remarks on ethanol oxidation by an "Acetobacter xylinum" microbial electrode (author's transl)'. In: *Ann Microbiol (Paris)* 126.2 (1975), pp. 175–186 (cited on page 8).

[48] Pranjal Chandra. 'Personalized biosensors for point-of-care diagnostics: from bench to bedside applications'. In: *Nanotheranostics* 7.2 (Feb. 9, 2023), pp. 210–215. DOI: 10.7150/ntno.81485. (Visited on 07/15/2023) (cited on pages 8, 9).

[49] H Ceren Ates et al. 'End-to-end design of wearable sensors'. In: *Nature Reviews Materials* 7.11 (2022), pp. 887–907 (cited on page 8).

[50] Santoshi U Singh et al. 'Advanced wearable biosensors for the detection of body fluids and exhaled breath by graphene'. In: *Microchimica Acta* 189.6 (2022), p. 236 (cited on page 8).

[51] Jean-Michel Kauffmann and Mila Pravda. 'THE ELECTROCHEMICAL BIOSENSOR ERA'. In: *Bioforum International* 2 (Jan. 1998), pp. 22–25 (cited on page 8).

[52] A. Pentland. 'Healthwear: medical technology becomes wearable'. In: *Computer* 37.5 (May 2004), pp. 42–49. DOI: 10.1109/MC.2004.1297238 (cited on page 8).

[53] Jayoung Kim et al. 'Wearable biosensors for healthcare monitoring'. In: *Nat Biotechnol* 37.4 (Apr. 2019), pp. 389–406. DOI: 10.1038/s41587-019-0045-y (cited on pages 8, 9).

[54] Jing Xu, Yunsheng Fang, and Jun Chen. 'Wearable Biosensors for Non-Invasive Sweat Diagnostics'. In: *Biosensors (Basel)* 11.8 (July 23, 2021), p. 245. DOI: 10.3390/bios11080245. (Visited on 07/16/2023) (cited on page 8).

[55] Chuanrui Chen, Shichao Ding, and Joseph Wang. 'Digital health for aging populations'. In: *Nat Med* 29.7 (July 2023), pp. 1623–1630. DOI: 10.1038/s41591-023-02391-8. (Visited on 07/19/2023) (cited on page 9).

[56] Ayodele T Odularu and Peter A Ajibade. 'Challenge of diabetes mellitus and researchers' contributions to its control'. In: *Open Chemistry* 19.1 (2021), pp. 614–634 (cited on page 9).

[57] Kerstin Rebrin et al. 'Subcutaneous glucose predicts plasma glucose independent of insulin: implications for continuous monitoring'. In: *American Journal of Physiology-Endocrinology and Metabolism* 277.3 (1999), E561–E571 (cited on page 9).

[58] Kimberly P. L. Chong et al. 'Consumer Perceptions of Wearable Technology Devices: Retrospective Review and Analysis'. In: *JMIR Mhealth Uhealth* 8.4 (Apr. 20, 2020), e17544. DOI: 10.2196/17544 (cited on page 9).

[59] Aaron Asael Smith, Rui Li, and Zion Tsz Ho Tse. 'Reshaping healthcare with wearable biosensors'. In: *Sci Rep* 13.1 (Mar. 27, 2023), p. 4998. DOI: 10.1038/s41598-022-26951-z. (Visited on 07/15/2023) (cited on page 9).

[60] Yingli Wang et al. 'Wearable plasmonic-metasurface sensor for noninvasive and universal molecular fingerprint detection on biointerfaces'. In: *Sci Adv* 7.4 (Jan. 2021), eabe4553. DOI: 10.1126/sciadv.abe4553 (cited on page 9).

[61] David C Klonoff, David Ahn, and Andjela Drincic. 'Continuous glucose monitoring: a review of the technology and clinical use'. In: *Diabetes Research and Clinical Practice* 133 (2017), pp. 178–192 (cited on page 9).

[62] Michael J Tierney et al. 'The GlucoWatch® biographer: a frequent, automatic and noninvasive glucose monitor'. In: *Annals of Medicine* 32.9 (2000), pp. 632–641 (cited on page 9).

[63] Prem C Pandey et al. 'Current advancements in transdermal biosensing and targeted drug delivery'. In: *Sensors* 19.5 (2019), p. 1028 (cited on page 9).
[64] Diabetes Research in Children Network (DirecNet) Study Group. 'Accuracy of the GlucoWatch G2 Biographer and the continuous glucose monitoring system during hypoglycemia: experience of the Diabetes Research in Children Network'. In: *Diabetes care* 27.3 (2004), pp. 722–726 (cited on page 9).
[65] Jayoung Kim et al. 'Simultaneous monitoring of sweat and interstitial fluid using a single wearable biosensor platform'. In: *Advanced Science* 5.10 (2018), p. 1800880 (cited on page 10).
[66] Jiangqi Zhao et al. 'A fully integrated and self-powered smartwatch for continuous sweat glucose monitoring'. In: *ACS sensors* 4.7 (2019), pp. 1925–1933 (cited on page 11).
[67] Anna Nguyen and John R White. 'FreeStyle Libre 3'. In: *Clinical Diabetes* 41.1 (2023), pp. 127–128 (cited on page 10).
[68] Inc Dexcom. *Dexcom G6 CGM system: No fingersticks, no scanning*. URL: https://www.dexcom.com/en-us/g6-cgm-system (cited on page 10).
[69] Medtronic. *Diabetes treatment - guardian sensor 3*. Oct. 2020. URL: https://www.medtronic.com/ca-en/diabetes/home/products/cgm-systems/guardian-sensor-3.html (cited on page 10).
[70] Shridhara Alva Karinka et al. '76-LB: Performance of FreeStyle Libre 3 System'. In: *Diabetes* (2022) (cited on page 10).
[71] Bo Wang et al. 'Wearable aptamer-field-effect transistor sensing system for noninvasive cortisol monitoring'. In: *Science advances* 8.1 (2022), eabk0967 (cited on pages 11, 12).
[72] Tianrui Chang et al. 'Highly integrated watch for noninvasive continual glucose monitoring'. In: *Microsystems & Nanoengineering* 8.1 (2022), p. 25 (cited on page 12).
[73] PKvitality. *K'Watch Glucose*. 2023. URL: https://www.pkvitality.com/ktrack-glucose/ (visited on 09/29/2023) (cited on page 12).
[74] PKvitality. *PKvitality – Bio-wearables Health Sport Home Page*. 2023. URL: https://www.pkvitality.com/ (visited on 09/29/2023) (cited on pages 12, 13).
[75] PKvitality. *K'Watch Athletes*. 2023. URL: https://www.pkvitality.com/ktrack-athlete/ (visited on 09/29/2023) (cited on page 12).
[76] Wilbert Villena Gonzales, Ahmed Toaha Mobashsher, and Amin Abbosh. 'The progress of glucose monitoring—A review of invasive to minimally and non-invasive techniques, devices and sensors'. In: *Sensors* 19.4 (2019), p. 800 (cited on page 13).
[77] Uirassu Borges Jr and Thomas Kubiak. 'Continuous glucose monitoring in type 1 diabetes: human factors and usage'. In: *Journal of diabetes science and technology* 10.3 (2016), pp. 633–639 (cited on page 13).

[78] Sung Sik Chu et al. 'Towards Multiplexed and Multimodal Biosensor Platforms in Real-Time Monitoring of Metabolic Disorders'. In: *Sensors* 22.14 (2022), p. 5200 (cited on page 13).

[79] Vivien Perrelle. *GitHub - DeVinci-Innovation-Center/BioWatch: A smartwatch for developing and implementing wearable sensors. — github.com*. https://github.com/DeVinci-Innovation-Center/BioWatch. Accessed 14-09-2023. 2022 (cited on pages 14, 33).

[80] Vivien Perrelle. *Vivien Perrelle - Creative Technologies Designer Student - Tutorials*. https://dvic.devinci.fr/member/vivien-perrelle#Tutorials. Accessed 14-09-2023. 2022 (cited on page 14).

[81] Nina Krey et al. 'Smartwatches: Accessory or Tool?: The Driving Force of Visibility and Usefulness'. In: (2016) (cited on page 15).

[82] *Infographic: Smartwatch 2021*. Counterpoint Research. Mar. 3, 2022. URL: https://www.counterpointresearch.com/infographic-smartwatch-2021/ (visited on 08/25/2023) (cited on page 15).

[83] *Smartwatch market share worldwide by vendor 2022*. Statista. URL: https://www.statista.com/statistics/1296818/smartwatch-market-share/ (visited on 08/25/2023) (cited on page 15).

[84] Aku Visuri et al. 'Quantifying sources and types of smartwatch usage sessions'. In: *Proceedings of the 2017 CHI Conference on Human Factors in Computing Systems*. 2017, pp. 3569–3581 (cited on page 15).

[85] Apple. *Apple Watch Series 9*. Accessed on September 29, 2023. URL: https://www.apple.com/fr/apple-watch-series-9/ (cited on page 15).

[86] Mordor Intelligence. *Smartwatch Market Size & Share Analysis - Growth Trends and Forecasts (2023 - 2028)*. Accessed on September 29, 2023. URL: https://www.mordorintelligence.com/industry-reports/smartwatch-market (cited on page 15).

[87] Rick Nelson. *IHS tears down Apple Watch, BOM less than 24% of MSRP*. Accessed on September 29, 2023. 2015. URL: https://www.electronicdesign.com/home/article/21205336/ihs-tears-down-apple-watch-bom-less-than-24-of-msrp (cited on page 16).

[88] Avnish Singh Jat and Tor-Morten Grønli. 'Smart watch for smart health monitoring: A literature review'. In: *International Work-Conference on Bioinformatics and Biomedical Engineering*. Springer. 2022, pp. 256–268 (cited on page 16).

[89] Nancy F Liu et al. 'Stigma in people with type 1 or type 2 diabetes'. In: *Clinical Diabetes* 35.1 (2017), pp. 27–34 (cited on page 16).

[90] Beata I Sińska et al. 'Identification of Sociodemographic and Clinical Factors Influencing the Feeling of Stigmatization in People with Type 1 Diabetes'. In: *Healthcare*. Vol. 11. 15. MDPI. 2023, p. 2185 (cited on page 16).

[91] Mark A. Sperling et al. 'CHAPTER 19 - Diabetes Mellitus'. In: *Pediatric Endocrinology (Fourth Edition)*. Ed. by Mark A. Sperling. Fourth Edition. W.B.

Saunders, 2014, 846–900.e1. DOI: 10.1016/B978-1-4557-4858-7.00028-7 (cited on page 16).

[92] Lena Hanberger et al. 'Needle-related pain, affective reactions, fear, and emotional coping in children and adolescents with type 1 diabetes: A cross-sectional study'. In: *Pain Management Nursing* 22.4 (2021), pp. 516–521 (cited on page 16).

[93] Laurel et al. Messer. 'Preserving Skin Integrity with Chronic Device Use in Diabetes'. In: *Diabetes Technol Ther* 22.4 (2018). DOI: 10.1089/dia.2018.0080 (cited on page 16).

[94] Lutz Heinemann and Edward Krisiunas. *Diabetes technology and waste: a complex problem piling up!* 2019 (cited on page 16).

[95] Jason Heikenfeld et al. 'Accessing analytes in biofluids for peripheral biochemical monitoring'. In: *Nature biotechnology* 37.4 (2019), pp. 407–419 (cited on pages 16, 39, 40, 45–47).

[96] Taehyun Ha et al. 'Examining user perceptions of smartwatch through dynamic topic modeling'. In: *Telematics Informatics* 34 (2017), pp. 1262–1273 (cited on page 17).

[97] Shadab Khan et al. 'An Optimized Artificial Intelligence System Using IoT Biosensors Networking for Healthcare Problems'. In: *Computational Intelligence and Neuroscience* 2022 (2022) (cited on page 17).

[98] Yihan Zhang et al. 'Wearable artificial intelligence biosensor networks'. In: *Biosensors and Bioelectronics* (2022), p. 114825 (cited on page 17).

[99] Xiaofeng Jin et al. 'Artificial intelligence biosensors for continuous glucose monitoring'. In: *Interdisciplinary Materials* 2.2 (2023), pp. 290–307 (cited on page 17).

[100] Yichao Zhao et al. 'A wearable freestanding electrochemical sensing system'. In: *Science advances* 6.12 (2020) (cited on page 17).

[101] National Science Foundation. *Adhesive film turns smartwatch into biochemical health monitoring system*. Accessed on September 29, 2023. 2020. URL: https://new.nsf.gov/news/adhesive-film-turns-smartwatch-biochemical-health#image-caption-credit-block (cited on page 17).

[102] Kubii. *Ecran rond LCD 1,28"*. https://www.kubii.com/fr/ecrans-supports/3242-ecran-rond-lcd-1-28-pouces-3272496305625.html. Accessed 14-09-2023 (cited on page 18).

[103] Zimmer&Peacock. *Technical Datasheet - Glucose Hypervalue Gen 1 Sensor*. Accessed 16-09-2023. 2023. URL: https://shop.zimmerpeacock.com/cdn/shop/files/TDS_Glucose_hypervalue_gen_1_v1.pdf?v=3365226608812840933 (cited on pages 28, 52).

[104] ZimmerPeacock. *Screen printed electrodes for biosensing - zimmerpeacocktech.com*. https://www.zimmerpeacocktech.com/knowledge-base/screen-printed-electrodes-for-biosensing/. Accessed 16-09-2023 (cited on page 29).

[105] ZimmerPeacock. *Introduction and review on screen printed electrodes (SPE) and their application to biosensors - youtube.com*. https://www.youtube.com/watch?v=Sm6sS-yuQgo. Accessed 16-09-2023. 2020 (cited on page 29).
[106] Zahra Taleat, Alireza Khoshroo, and Mohammad Mazloum-Ardakani. 'Screen-printed electrodes for biosensing: A review (2008–2013)'. In: *Microchimica Acta* 181 (2014), pp. 865–891 (cited on page 29).
[107] ZimmerPeacock. *Glucose to API - zimmerpeacocktech.com*. https://www.zimmerpeacocktech.com/products/glucose-sensors/. Accessed 16-09-2023 (cited on page 29).
[108] Seyyed Hossein Khatami et al. 'Glucose oxidase: Applications, sources, and recombinant production'. In: *Biotechnology and Applied Biochemistry* (2021) (cited on page 29).
[109] Zhimin Tao et al. 'Kinetic studies on enzyme-catalyzed reactions: Oxidation of glucose, decomposition of hydrogen peroxide and their combination'. In: *Biophysical journal* 96.7 (2009), pp. 2977–2988 (cited on page 29).
[110] James Powers Martin Peacock Sindre Sopstad. *Hybrid electrochemical sensor platform - Wearable platform suitable for CGM* (cited on page 29).
[111] Zimmer & Peacock Ltd. *ecFlex quick-start developer guide* (cited on pages 29, 31, 32).
[112] BrightVolt. *BrightVolt Solid State Batteries - brightvolt.com*. https://www.brightvolt.com/our-technology/. Accessed 16-09-2023 (cited on pages 29, 30).
[113] ZimmerandPeacock. *Products - zimmerpeacocktech.com*. https://www.zimmerpeacocktech.com/products/. Accessed 14-09-2023. 2020 (cited on page 30).
[114] Christopher Legner et al. 'Sweat sensing in the smart wearables era: Towards integrative, multifunctional and body-compliant perspiration analysis'. In: *Sensors and Actuators A: Physical* 296 (2019), pp. 200–221. DOI: https://doi.org/10.1016/j.sna.2019.07.020 (cited on page 30).
[115] Amay J Bandodkar et al. 'Wearable sensors for biochemical sweat analysis'. In: *Annual Review of Analytical Chemistry* 12 (2019), pp. 1–22 (cited on page 30).
[116] Miroslav Pohanka. 'Screen Printed Electrodes in Biosensors and Bioassays'. In: *A Review. Int. J. Electrochem. Sci* 15 (2020), pp. 11024–11035 (cited on page 30).
[117] Python. *Bleak* (cited on page 31).
[118] Guillaume Celosia and Mathieu Cunche. 'Fingerprinting bluetooth-low-energy devices based on the generic attribute profile'. In: *Proceedings of the 2nd International ACM Workshop on Security and Privacy for the Internet-of-Things*. 2019, pp. 24–31 (cited on page 31).
[119] Pallets projects. *Flask* (cited on page 32).
[120] Python. *sqlite3* (cited on page 33).

[121] Xiaolu Li et al. 'Lactate metabolism in human health and disease'. In: *Signal transduction and targeted therapy* 7.1 (2022), p. 305 (cited on page 37).
[122] Christopher D Foucher and Robert E Tubben. 'Lactic acidosis'. In: *StatPearls [Internet*. StatPearls Publishing, 2022 (cited on page 37).
[123] J. C. Goodman et al. 'Extracellular lactate and glucose alterations in the brain after head injury measured by microdialysis'. In: *Critical Care Medicine* 27.9 (Sept. 1999), pp. 1965–1973. DOI: 10.1097/00003246-199909000-00041 (cited on page 37).
[124] Fahmida Alam et al. 'Lactate biosensing: The emerging point-of-care and personal health monitoring'. In: *Biosensors and Bioelectronics* 117 (Oct. 15, 2018), pp. 818–829. DOI: 10.1016/j.bios.2018.06.054. (Visited on 09/07/2023) (cited on page 37).
[125] Ayesha M. F. Heinis et al. 'Comparison of two point-of-care testing (POCT) devices for fetal lactate during labor'. In: *Clinical Chemistry and Laboratory Medicine* 50.1 (Sept. 29, 2011), pp. 89–93. DOI: 10.1515/CCLM.2011.734 (cited on page 37).
[126] Itzhak Brook. 'The importance of lactic acid levels in body fluids in the detection of bacterial infections'. In: *Reviews of Infectious Diseases* 3.3 (1981), pp. 470–478 (cited on page 37).
[127] S. Walenta et al. 'High lactate levels predict likelihood of metastases, tumor recurrence, and restricted patient survival in human cervical cancers'. In: *Cancer Research* 60.4 (Feb. 15, 2000), pp. 916–921 (cited on page 37).
[128] Elizabeth L. Cureton et al. 'A different view of lactate in trauma patients: protecting the injured brain'. In: *The Journal of Surgical Research* 159.1 (Mar. 2010), pp. 468–473. DOI: 10.1016/j.jss.2009.04.020 (cited on page 37).
[129] Matthew L Goodwin et al. 'Blood lactate measurements and analysis during exercise: a guide for clinicians'. In: *Journal of diabetes science and technology* 1.4 (2007), pp. 558–569 (cited on pages 37, 38, 41, 43, 44).
[130] I. Jacobs. 'Blood lactate. Implications for training and sports performance'. In: *Sports Medicine (Auckland, N.Z.)* 3.1 (1986), pp. 10–25. DOI: 10.2165/00007256-198603010-00003 (cited on page 37).
[131] HR Gosker and AMWJ Schols. *Fatigued muscles in COPD but no finishing line in sight*. 2008 (cited on page 37).
[132] Simeon P Cairns. 'Lactic acid and exercise performance'. In: *Sports medicine* 36.4 (2006), pp. 279–291 (cited on pages 38, 43).
[133] L Messonnier and H Dubouchaud. 'Le lactate: sa cinétique, son métabolisme, ses relations avec la performance et ses controverses'. In: *Science & Motricité* 70 (2010), pp. 21–30 (cited on page 38).
[134] Bente Klarlund Pedersen, Adam Steensberg, and Peter Schjerling. 'Exercise and interleukin-6'. In: *Current opinion in hematology* 8.3 (2001), pp. 137–141 (cited on page 38).

[135] Josef Finsterer. 'Biomarkers of peripheral muscle fatigue during exercise'. In: *BMC musculoskeletal disorders* 13.1 (2012), pp. 1–13 (cited on page 38).

[136] Jing-jing Wan et al. 'Muscle fatigue: general understanding and treatment'. In: *Experimental & molecular medicine* 49.10 (2017), e384–e384 (cited on page 38).

[137] George Theofilidis et al. 'Monitoring exercise-induced muscle fatigue and adaptations: making sense of popular or emerging indices and biomarkers'. In: *Sports* 6.4 (2018), p. 153 (cited on page 38).

[138] L Véronique Billat. 'Use of blood lactate measurements for prediction of exercise performance and for control of training'. In: *Sports medicine* 22.3 (1996), pp. 157–175 (cited on page 38).

[139] D. B. Pyne et al. 'Evaluation of the Lactate Pro blood lactate analyser'. In: *European Journal of Applied Physiology* 82.1 (May 2000), pp. 112–116. DOI: 10.1007/s004210050659 (cited on page 38).

[140] Jacinta M. Bonaventura et al. 'Reliability and Accuracy of Six Hand-Held Blood Lactate Analysers'. In: *Journal of Sports Science & Medicine* 14.1 (Jan. 27, 2015), pp. 203–214. (Visited on 09/07/2023) (cited on page 38).

[141] Halil İbrahim Kaya et al. 'İki Farkli Taşinabilir Elektro-Enzimatik Laktat Analiz Cihazinin Geçerlilik ve Güvenilirlik Çalişmasi'. In: *Spor Hekimligi Dergisi* 55.2 (2020). Publisher: Türkiye Spor Hekimleri Dernegi, pp. 138–147. DOI: 10.5152/tjsm.2020.170. (Visited on 09/07/2023) (cited on page 38).

[142] Julia Madden et al. 'Biosensing in dermal interstitial fluid using microneedle based electrochemical devices'. In: *Sensing and Bio-Sensing Research* 29 (2020), p. 100348 (cited on page 38).

[143] Xing Xuan et al. 'Lactate biosensing for reliable on-body sweat analysis'. In: *ACS sensors* 6.7 (2021), pp. 2763–2771 (cited on page 38).

[144] Wei Gao, George A Brooks, and David C Klonoff. 'Wearable physiological systems and technologies for metabolic monitoring'. In: *Journal of applied physiology* 124.3 (2018), pp. 548–556 (cited on page 38).

[145] P Dardano, I Rea, and L De Stefano. 'Microneedles-based electrochemical sensors: New tools for advanced biosensing'. In: *Current Opinion in Electrochemistry* 17 (2019), pp. 121–127 (cited on page 38).

[146] Misagh Rezapour Sarabi, Sattar Akbari Nakhjavani, and Savas Tasoglu. '3D-Printed Microneedles for Point-of-Care Biosensing Applications'. In: *Micromachines* 13.7 (July 13, 2022), p. 1099. DOI: 10.3390/mi13071099. (Visited on 09/07/2023) (cited on pages 38, 39).

[147] Apoorva Panda et al. 'Fabrication and development of controlled release PLGA microneedles for macromolecular delivery using FITC-Dextran as model molecule'. In: *Journal of Drug Delivery Science and Technology* 68 (Feb. 2022), p. 102712. DOI: 10.1016/j.jddst.2021.102712 (cited on page 39).

[148] Boyu Qin et al. 'Porosity control of polylactic acid porous microneedles using microfluidic technology'. In: *2022 IEEE CPMT Symposium Japan (ICSJ)*

(Nov. 9, 2022), pp. 127–130. DOI: 10.1109/ICSJ55786.2022.10034733 (cited on page 39).
[149] Letizia Ventrelli, Lucanos Marsilio Strambini, and Giuseppe Barillaro. 'Microneedles for transdermal biosensing: current picture and future direction'. In: *Advanced healthcare materials* 4.17 (2015), pp. 2606–2640 (cited on page 39).
[150] Mark Friedel et al. 'Opportunities and challenges in the diagnostic utility of dermal interstitial fluid'. In: *Nature Biomedical Engineering* (2023), pp. 1–15 (cited on page 39).
[151] D Barry Keenan et al. 'Interstitial fluid glucose time-lag correction for real-time continuous glucose monitoring'. In: *Biomedical signal processing and control* 8.1 (2013), pp. 81–89 (cited on page 39).
[152] Robert M Califf. 'Biomarker definitions and their applications'. In: *Experimental Biology and Medicine* 243.3 (2018), pp. 213–221 (cited on page 40).
[153] John A Wagner. 'Overview of biomarkers and surrogate endpoints in drug development'. In: *Disease markers* 18.2 (2002), pp. 41–46 (cited on page 40).
[154] Boyu Zhu et al. 'An overview of wearable and implantable electrochemical glucose sensors'. In: *Electroanalysis* 34.2 (2022), pp. 237–245 (cited on page 40).
[155] National Center for Biotechnology Information. 'PubChem Compound Summary for CID 91435, Lactate'. In: (). Consulted on August 18, 2022 (cited on pages 40, 41).
[156] Joshua D Rabinowitz and Sven Enerbäck. 'Lactate: the ugly duckling of energy metabolism'. In: *Nature Metabolism* 2.7 (2020), pp. 566–571 (cited on page 40).
[157] Zhou Zhou, Ming-Jiang Xu, and Bin Gao. 'Hepatocytes: a key cell type for innate immunity'. In: *Cellular & molecular immunology* 13.3 (2016), pp. 301–315 (cited on page 41).
[158] Barrie Phypers and JM Tom Pierce. 'Lactate physiology in health and disease'. In: *Continuing Education in Anaesthesia, Critical Care and Pain* 6.3 (2006), pp. 128–132 (cited on pages 41, 42).
[159] Pierre J Magistretti and Igor Allaman. 'Lactate in the brain: from metabolic end-product to signalling molecule'. In: *Nature Reviews Neuroscience* 19.4 (2018), pp. 235–249 (cited on page 41).
[160] Miroslav Pohanka. 'D-lactic acid as a metabolite: toxicology, diagnosis, and detection'. In: *BioMed Research International* 2020 (2020) (cited on page 41).
[161] Shui Ping Wang et al. 'Pivotal roles for pH, lactate, and lactate-utilizing bacteria in the stability of a human colonic microbial ecosystem'. In: *Msystems* 5.5 (2020), e00645–20 (cited on page 41).
[162] Alain L Servin. 'Antagonistic activities of lactobacilli and bifidobacteria against microbial pathogens'. In: *FEMS microbiology reviews* 28.4 (2004), pp. 405–440 (cited on page 41).

[163] Satish K Tuteja, Connor Ormsby, and Suresh Neethirajan. 'Noninvasive label-free detection of cortisol and lactate using graphene embedded screen-printed electrode'. In: *Nano-micro letters* 10.3 (2018), pp. 1–10 (cited on page 41).
[164] Kamel S Kamel, Man S Oh, and Mitchell L Halperin. 'L-lactic acidosis: pathophysiology, classification, and causes; emphasis on biochemical and metabolic basis'. In: *Kidney International* 97.1 (2020), pp. 75–88 (cited on page 41).
[165] Francesca Miranda Di Mauro and Gretchen Lee Schoeffler. 'Point of care measurement of lactate'. In: *Topics in companion animal medicine* 31.1 (2016), pp. 35–43 (cited on page 41).
[166] Michael Dacko and Thomas Lange. 'Improved detection of lactate and β-hydroxybutyrate using MEGA-sLASER at 3 T'. In: *NMR in Biomedicine* 32.7 (2019), e4100 (cited on page 41).
[167] Jan P. Kovacic. 'Chapter 60 - Lactic Acidosis'. In: (2009), pp. 254–257. DOI: 10.1016/B978-1-4160-2591-7.10060-8 (cited on pages 41, 42).
[168] Erin Hopkins, Terrence Sanvictores, and Sandeep Sharma. 'Physiology, acid base balance'. In: *StatPearls [Internet*. StatPearls Publishing, 2021 (cited on page 41).
[169] GW Mainwood and JM Renaud. 'The effect of acid–base balance on fatigue of skeletal muscle'. In: *Canadian journal of physiology and pharmacology* 63.5 (1985), pp. 403–416 (cited on page 41).
[170] Anne Waugh, Allison Grant, Janet S Ross, et al. *Ross and Wilson anatomy and physiology in health and illness*. Churchill livingstone, 2002 (cited on page 41).
[171] Jessica N Hinojosa, Christopher M Hearon, and Robert J Kowalsky. 'Blood lactate response to active recovery in athletes vs. non-athletes'. In: *Sport Sciences for Health* 17.3 (2021), pp. 699–705 (cited on page 41).
[172] Jacob Dunn and Michael H Grider. 'Physiology, adenosine triphosphate'. In: *StatPearls [Internet*. StatPearls Publishing, 2021 (cited on page 42).
[173] Shaohui Huang and Michael P Czech. 'The GLUT4 glucose transporter'. In: *Cell metabolism* 5.4 (2007), pp. 237–252 (cited on page 41).
[174] American Chemical Society National Historic Chemical Landmarks. *Carl and Gerty Cori and Carbohydrate Metabolism*. Accessed on July 24th, 2022 (cited on page 42).
[175] *How anaerobic metabolism still contributes to VO2?* Accessed on July 26th, 2022 (cited on page 42).
[176] K Sahlin et al. 'Effects of lactic acid accumulation and ATP decrease on muscle tension and relaxation'. In: *American Journal of Physiology-Cell Physiology* 240.3 (1981), pp. C121–C126 (cited on page 42).
[177] Robert A Robergs, Farzenah Ghiasvand, and Daryl Parker. 'Biochemistry of exercise-induced metabolic acidosis'. In: *American Journal of Physiology-Regulatory, Integrative and Comparative Physiology* (2004) (cited on page 42).

[178] Gerrit Van Hall. 'Lactate kinetics in human tissues at rest and during exercise'. In: *Acta physiologica* 199.4 (2010), pp. 499–508 (cited on pages 42, 43, 46).
[179] Sean M Forsythe and Gregory A Schmidt. 'Sodium bicarbonate for the treatment of lactic acidosis'. In: *Chest* 117.1 (2000), pp. 260–267 (cited on page 43).
[180] Jeffrey A Kraut and Nicolaos E Madias. 'Lactic acidosis'. In: *New England Journal of Medicine* 371.24 (2014), pp. 2309–2319 (cited on page 42).
[181] Nicolaos E Madias. 'Lactic acidosis'. In: *Kidney international* 29.3 (1986), pp. 752–774 (cited on page 42).
[182] Andrew P Halestrap and Marieangela C Wilson. 'The monocarboxylate transporter family—role and regulation'. In: *IUBMB life* 64.2 (2012), pp. 109–119 (cited on page 43).
[183] KJ McCullagh et al. 'Role of the lactate transporter (MCT1) in skeletal muscles'. In: *American Journal of Physiology-Endocrinology And Metabolism* 271.1 (1996), E143–E150 (cited on page 42).
[184] RL Hazelwood. 'Carbohydrate metabolism'. In: *Avian physiology*. Springer, 1986, pp. 303–325 (cited on page 42).
[185] GA Brooks. 'Lactate production under fully aerobic conditions: the lactate shuttle during rest and exercise.' In: *Federation proceedings*. Vol. 45. 13. 1986, pp. 2924–2929 (cited on page 42).
[186] A t Katz and K Sahlin. 'Regulation of lactic acid production during exercise'. In: *Journal of applied physiology* 65.2 (1988), pp. 509–518 (cited on page 42).
[187] F Carré. 'Répartition du lactate dans l'organisme après un exercice musculaire: le modèle historique unicompartimental et ses limites'. In: *Science & sports* 8.3 (1993), pp. 189–191 (cited on pages 42, 43).
[188] H Freund and P Zouloumian. 'Lactate after exercise in man: I. Evolution kinetics in arterial blood'. In: *European Journal of Applied Physiology and Occupational Physiology* 46.2 (1981), pp. 121–133 (cited on pages 42, 43).
[189] P Zouloumian and H Freund. 'Lactate after exercise in Man: II. Mathematical model.' In: *European journal of applied physiology and occupational physiology* 46.2 (1981), pp. 135–147 (cited on pages 42, 43).
[190] P Zouloumian and H Freund. 'Lactate after exercise in man: III. Properties of the compartment model'. In: *European Journal of Applied Physiology and Occupational Physiology* 46.2 (1981), pp. 149–160 (cited on pages 42, 43).
[191] H Freund and P Zouloumian. 'Lactate after exercise in man: IV. Physiological observations and model predictions'. In: *European Journal of Applied Physiology and Occupational Physiology* 46.2 (1981), pp. 161–176 (cited on pages 42, 43).
[192] A Zerman, C Cobelli, and L Sacca. 'A Compartmental Model Of Lactate Kinetics In Humans: Role Of Sites Of Tracer Administration And Sampling'. In: *[1990] Proceedings of the Twelfth Annual International Conference of the IEEE*

Engineering in Medicine and Biology Society. IEEE. 1990, pp. 959–960 (cited on pages 42, 43).

[193] Ralph Beneke, Masen D Jumah, and Renate M Leithäuser. 'Modelling the lactate response to short-term all out exercise'. In: *Dynamic medicine* 6.1 (2007), pp. 1–7 (cited on pages 42, 43).

[194] John F Moxnes and Øyvind Sandbakk. 'The kinetics of lactate production and removal during whole-body exercise'. In: *Theoretical Biology and Medical Modelling* 9.1 (2012), pp. 1–14 (cited on pages 42, 43).

[195] George A Brooks. 'Anaerobic threshold: review of the concept and directions for future research.' In: *Medicine and science in sports and exercise* 17.1 (1985), pp. 22–34 (cited on page 43).

[196] HERBERT Löllgen, TERRY Graham, and GISELA Sjogaard. 'Muscle metabolites, force, and perceived exertion bicycling at varying pedal rates'. In: *Med Sci Sports Exerc* 12.5 (1980), pp. 345–51 (cited on page 44).

[197] L Bruce Gladden. 'Lactate metabolism during exercise'. In: *MEDICINE AND SPORT SCIENCE* 46 (2004), pp. 152–196 (cited on page 44).

[198] J Karlsson, B Diamant, and B Saltin. 'Muscle metabolites during submaximal and maximal exercise in man'. In: *Scandinavian journal of clinical and laboratory investigation* 26.4 (1970), pp. 385–394 (cited on page 44).

[199] Ira Jacobs and Peter Kaiser. 'Lactate in blood, mixed skeletal muscle, and FT or ST fibres during cycle exercise in man'. In: *Acta physiologica scandinavica* 114.3 (1982), pp. 461–466 (cited on page 44).

[200] Michael J Buono and John E Yeager. 'Intraerythrocyte and plasma lactate concentrations during exercise in humans'. In: *European journal of applied physiology and occupational physiology* 55.3 (1986), pp. 326–329 (cited on page 44).

[201] ROBERT T Harris and GARY A Dudley. 'Exercise alters the distribution of ammonia and lactate in blood'. In: *Journal of Applied Physiology* 66.1 (1989), pp. 313–317 (cited on page 44).

[202] Peter Foxdal et al. 'Lactate concentration differences in plasma, whole blood, capillary finger blood and erythrocytes during submaximal graded exercise in humans'. In: *European Journal of Applied Physiology and Occupational Physiology* 61.3 (1990), pp. 218–222 (cited on page 44).

[203] EDITH W Smith et al. 'Lactate distribution in the blood during progressive exercise.' In: *Medicine and science in sports and exercise* 29.5 (1997), pp. 654–660 (cited on page 44).

[204] Carsten Juel et al. 'Lactate and potassium fluxes from human skeletal muscle during and after intense, dynamic, knee extensor exercise'. In: *Acta physiologica Scandinavica* 140.2 (1990), pp. 147–159 (cited on page 44).

[205] Narendra Kotwal and Aditi Pandit. 'Variability of capillary blood glucose monitoring measured on home glucose monitoring devices'. In: *Indian journal of endocrinology and metabolism* 16.Suppl 2 (2012), S248 (cited on page 44).
[206] Hye Soon Kim. 'Blood glucose measurement: is serum equal to plasma?' In: *Diabetes & Metabolism Journal* 40.5 (2016), pp. 365–366 (cited on page 44).
[207] A REETA PÖSÖ, KIMMO J LAMPINEN, and LEENA A RÄSÄNEN. 'Distribution of lactate between red blood cells and plasma after exercise'. In: *Equine Veterinary Journal* 27.S18 (1995), pp. 231–234 (cited on page 44).
[208] NM Koho, LK Väihkönen, and AR Pösö. 'Lactate transport in red blood cells by monocarboxylate transporters'. In: *Equine Veterinary Journal* 34.S34 (2002), pp. 555–559 (cited on page 44).
[209] JR Williams, N Armstrong, and BJ Kirby. 'The influence of the site of sampling and assay medium upon the measurement and interpretation of blood lactate responses to exercise'. In: *Journal of sports sciences* 10.2 (1992), pp. 95–107 (cited on pages 44, 45).
[210] S Oyono-Enguelle et al. 'Comparison of arterial and venous blood lactate kinetics after short exercise'. In: *International journal of sports medicine* 10.01 (1989), pp. 16–24 (cited on page 44).
[211] Chris Higgins. *Lactate measurement: arterial versus venous blood sampling*. January 2017. Accessed on August 17, 2022 (cited on page 44).
[212] Olivier Collange et al. 'Comparison of capillary and arterial lactate levels in patients with shock'. In: *Anaesthesia Critical Care & Pain Medicine* 36.3 (2017), pp. 157–162 (cited on page 44).
[213] Leandro Seoane et al. 'Capillary lactic acid validation in an ED'. In: *The American journal of emergency medicine* 31.9 (2013), pp. 1365–1367 (cited on page 44).
[214] Anette Raa et al. 'Validation of a point-of-care capillary lactate measuring device (Lactate Pro 2)'. In: *Scandinavian journal of trauma, resuscitation and emergency medicine* 28.1 (2020), pp. 1–7 (cited on page 44).
[215] Colin A Graham et al. 'Agreement between capillary and venous lactate in emergency department patients: prospective observational study'. In: *BMJ open* 9.4 (2019), e026109 (cited on page 44).
[216] David Stoll et al. 'Capillary and venous lactate measurements with a handheld device compared to venous blood-gas analysis for emergency patients'. In: *Scandinavian Journal of Trauma, Resuscitation and Emergency Medicine* 26.1 (2018), pp. 1–5 (cited on page 44).
[217] Pattharawin Pattharanitima et al. 'Correlation of arterial, central venous and capillary lactate levels in septic shock patients'. In: *Journal of the Medical Association of Thailand* 94.2 (2011), p. 175 (cited on page 45).
[218] Bryan Lightowler and Anthony Hoswell. 'Can handheld POC capillary lactate measurement be used with arterial and venous laboratory testing

methods in the identification of sepsis?' In: *Journal of Paramedic Practice* 8.8 (2016), pp. 396–406 (cited on page 45).

[219] Jacinta M Bonaventura et al. 'Reliability and accuracy of six hand-held blood lactate analysers'. In: *Journal of sports science & medicine* 14.1 (2015), p. 203 (cited on page 45).

[220] Robert Ahmun et al. 'Criterion validity of the lactate Pro LT-1710 portable analyser'. In: *Journal of Sports Sciences* 20.1 (2002), p. 31 (cited on page 45).

[221] Sachiko Ono, Gyohei Egawa, and Kenji Kabashima. 'Regulation of blood vascular permeability in the skin'. In: *Inflammation and regeneration* 37.1 (2017), pp. 1–8 (cited on page 45).

[222] John F Currie, Michael M Bodo, and Frederick J Pearce. *Novel Non-Intrusive Trans-Dermal Remote Wireless Micro-Fluidic Monitoring System Applied to Continuous Glucose and Lactate Assays for Casualty Care and Combat Readiness Assessment*. Tech. rep. Walter Reed Army Institute Of Research, 2004 (cited on page 45).

[223] PA Jansson, ANNE LENE Krogstad, and P Lonnroth. 'Microdialysis measurements in skin: evidence for significant lactate release in healthy humans'. In: *American Journal of Physiology-Endocrinology And Metabolism* 271.1 (1996), E138–E142 (cited on pages 45, 46).

[224] T Ohkuwa et al. 'The Relationship between Exercise Intensity and Lactate Concentration on the Skin Surface.' In: *International Journal of Biomedical Science: IJBS* 5.1 (2009), pp. 23–27 (cited on page 46).

[225] F Birklein, M Weber, and B Neundörfer. 'Increased skin lactate in complex regional pain syndrome: evidence for tissue hypoxia?' In: *Neurology* 55.8 (2000), pp. 1213–1215 (cited on page 45).

[226] M Muller et al. 'Measurement of interstitial muscle glucose and lactate concentrations during an oral glucose tolerance test'. In: *American Journal of Physiology-Endocrinology And Metabolism* 271.6 (1996), E1003–E1007 (cited on page 45).

[227] Röcker K Ahlgrim C Prettin S. 'Blood lactate levels at rest: Normal values and association with predominant type of exercise'. In: Berlin, Oct. 2012, pp. 7–8 (cited on page 45).

[228] Damien K Ming et al. 'Real-time continuous measurement of lactate through a minimally invasive microneedle patch: a phase I clinical study'. In: *BMJ Innovations* 8.2 (2022) (cited on page 46).

[229] Ming-Nan Chien et al. 'Continuous Lactate Monitoring System Based on Percutaneous Microneedle Array'. In: *Sensors* 22.4 (2022), p. 1468 (cited on pages 46–48).

[230] Irwin M Braverman. 'The cutaneous microcirculation'. In: 5.1 (2000), pp. 3–9 (cited on page 46).

[231] AL Krogstad et al. 'Microdialysis methodology for the measurement of dermal interstitial fluid in humans'. In: *British Journal of Dermatology* 134.6 (1996), pp. 1005–1012 (cited on page 46).

[232] Anna-Maria Spehar-Délèze, Salzitsa Anastasova, and Pankaj Vadgama. 'Monitoring of lactate in interstitial fluid, saliva and sweat by electrochemical biosensor: the uncertainties of biological interpretation'. In: *Chemosensors* 9.8 (2021), p. 195 (cited on page 47).

[233] A Caliò et al. 'Polymeric microneedles based enzymatic electrodes for electrochemical biosensing of glucose and lactic acid'. In: *Sensors and Actuators B: Chemical* 236 (2016), pp. 343–349 (cited on page 47).

[234] Paolo Bollella et al. 'Microneedle-based biosensor for minimally-invasive lactate detection'. In: *Biosensors and Bioelectronics* 123 (2019), pp. 152–159 (cited on pages 47, 48).

[235] Paolo Bollella et al. 'Minimally-invasive microneedle-based biosensor array for simultaneous lactate and glucose monitoring in artificial interstitial fluid'. In: *Electroanalysis* 31.2 (2019), pp. 374–382 (cited on page 48).

[236] Noémie Elgrishi et al. 'A practical beginner's guide to cyclic voltammetry'. In: *Journal of chemical education* 95.2 (2018), pp. 197–206 (cited on page 48).

[237] Aaron A Rowe et al. 'Cheapstat: An open-source,"do-it-yourself" potentiostat for analytical and educational applications'. In: *PloS one* 6.9 (2011), e23783 (cited on page 49).

[238] J. M. West. 'Applications of Potentiostats in Corrosion Studies'. In: *British Corrosion Journal* 5.2 (1970), pp. 65–71. DOI: 10.1179/000705970798324810 (cited on page 49).

[239] Chun-Yueh Huang. 'Design of a voltammetry potentiostat for biochemical sensors'. In: *Analog Integrated Circuits and Signal Processing* 67 (2011), pp. 375–381 (cited on page 49).

[240] Manoj B Kale et al. 'Electrocatalysts by electrodeposition: recent advances, synthesis methods, and applications in energy conversion'. In: *Advanced Functional Materials* 31.25 (2021), p. 2101313 (cited on page 49).

[241] Hanna Sopha and Jan M. Macák. 'Bipolar Electrochemistry for the Synthesis of Anodic TiO2 Nanotube Layers'. In: *ECS Meeting Abstracts* (2022) (cited on page 49).

[242] Allison V Cordova-Huaman, Victor R Jauja-Ccana, and Adolfo La Rosa-Toro. 'Low-cost smartphone-controlled potentiostat based on Arduino for teaching electrochemistry fundamentals and applications'. In: *Heliyon* 7.2 (2021) (cited on page 49).

[243] Andrew J Wain and Edmund JF Dickinson. 'Nanoscale characteristics of electrochemical systems'. In: *Frontiers of Nanoscience*. Vol. 18. Elsevier, 2021, pp. 1–48 (cited on page 49).

[244] PalmSens. *MultiEmStat 3 amp; 3+*. 2021. URL: https://www.palmsens.com/app/uploads/2020/04/MultiEmStat3-and-3-description.pdf (cited on page 49).
[245] *LMP91000 data sheet, product information and support - TI.com — ti.com*. https://www.ti.com/product/LMP91000. Accessed 14-09-2023 (cited on page 49).
[246] *Software - PalmSens - palmsens.com*. https://www.palmsens.com/software/. Accessed 14-09-2023 (cited on page 49).
[247] Texas Instruments. *LMP91000 Sensor AFE Software - Download*. Accessed on September 22, 2023. 2012 (cited on pages 49, 50).
[248] *LMP91000 data sheet, product information and support | TI.com*. URL: https://www.ti.com/product/LMP91000 (visited on 09/09/2023) (cited on page 50).
[249] Antonio Vincenzo Radogna et al. 'ElectroSense: a Low-cost Wearable Potentiostat for Real-time Monitoring of Glucose Level'. In: *2023 8th International Conference on Smart and Sustainable Technologies (SpliTech)*. IEEE. 2023, pp. 1–5 (cited on page 51).
[250] Yanxiang Cheng et al. 'A touch-actuated glucose sensor fully integrated with microneedle array and reverse iontophoresis for diabetes monitoring'. In: *Biosensors and Bioelectronics* 203 (2022), p. 114026 (cited on page 51).
[251] Maria A Komkova et al. 'Simultaneous monitoring of sweat lactate content and sweat secretion rate by wearable remote biosensors'. In: *Biosensors and Bioelectronics* 202 (2022), p. 113970 (cited on page 51).
[252] Mikio Yamada et al. 'Wristwatch Biosensor for Sweat Lactic Acid Monitoring'. In: *2022 IEEE 35th International Conference on Micro Electro Mechanical Systems Conference (MEMS)*. IEEE. 2022, pp. 289–292 (cited on page 51).
[253] Hiroyuki Kudo, Takuya Shibahara, and Yoshiki Tojyo. 'Salivary uric acid sensor using the fordable "Finger-Powered" microfluidic device'. In: *Electronics and Communications in Japan* 105.3 (2022), e12363 (cited on page 51).
[254] Chi Tran Nhu et al. 'Development of a miniaturised potentiostat for urea detection using the LMP91000'. In: *Vietnam Journal of Science, Technology and Engineering* 65.1 (2023), pp. 19–24 (cited on page 51).
[255] Muhammad Afiq Abdul Ghani et al. 'Portable electrochemical biosensors based on microcontrollers for detection of viruses: a review'. In: *Biosensors* 12.8 (2022), p. 666 (cited on page 51).
[256] Karim Kaci et al. 'Paving the way to point of care (POC) devices for SARS-CoV-2 detection'. In: *Talanta* 247 (2022), p. 123542 (cited on page 51).
[257] Alper Demirhan et al. 'Low-Cost High-Resolution Potentiostat for Electrochemical Detection of Nucleic Acids and Biomolecular Interactions'. In: *Micromachines* 13.10 (2022), p. 1610 (cited on page 51).

[258] Alex Whipple et al. 'A fully flexible handheld wireless estrogen sensing device'. In: *2022 IEEE International Conference on Flexible and Printable Sensors and Systems (FLEPS)*. IEEE. 2022, pp. 1–4 (cited on page 51).

[259] Joydeep Mahato, C Retna Raj, and Karabi Biswas. 'Low-noise potentiostat circuit for electrochemical detection of heavy metals or metalloids'. In: *IEEE Transactions on Instrumentation and Measurement* 71 (2022), pp. 1–9 (cited on page 51).

[260] Valentina Bianchi et al. 'A Wi-Fi cloud-based portable potentiostat for electrochemical biosensors'. In: *IEEE Transactions on Instrumentation and Measurement* 69.6 (2019), pp. 3232–3240 (cited on page 51).

[261] Orlando S Hoilett et al. 'KickStat: A coin-sized potentiostat for high-resolution electrochemical analysis'. In: *Sensors* 20.8 (2020), p. 2407 (cited on page 51).

[262] Shawn Chia-Hung Lee and Peter J Burke. 'NanoStat: An open source, fully wireless potentiostat'. In: *Electrochimica Acta* 422 (2022), p. 140481 (cited on page 51).

[263] Vijayalaxmi Manoharan et al. 'Platform-agnostic electrochemical sensing app and companion potentiostat'. In: *Analyst* (2023) (cited on page 51).

[264] Zimmer&Peacock. *Electro-Analytical Techniques*. URL: https://www.zimmerpeacocktech.com/knowledge-base/faq/electro-analytical-techniques/ (visited on 09/09/2023) (cited on page 52).

[265] OJ Guy and KAD Walker. 'Chapter 4-Graphene Functionalization for Biosensor Applications. Silicon Carbide Biotechnol. 2016'. In: *DOI* 10 (), pp. 85–141 (cited on page 52).

[266] LinnesLab. *GitHub - LinnesLab/LMP91000: Arduino library for the LMP91000 AFE Potentiostat for Electrochemical Sensing - github.com*. https://github.com/LinnesLab/LMP91000. Accessed 15-09-2023 (cited on page 52).

[267] Fahmida Alam et al. 'Lactate biosensing: The emerging point-of-care and personal health monitoring'. In: *Biosensors and Bioelectronics* 117 (2018), pp. 818–829 (cited on page 52).

[268] *Vrttlkkfe - Fil de platine 99,99 % pur - amazon.fr*. Accessed 15-09-2023 (cited on page 52).

[269] Han Yu et al. 'Recent progress of the practical applications of the platinum nanoparticle-based electrochemistry biosensors'. In: *Frontiers in Chemistry* 9 (2021), p. 677876 (cited on page 52).

[270] Xia Chu et al. 'Amperometric glucose biosensor based on electrodeposition of platinum nanoparticles onto covalently immobilized carbon nanotube electrode'. In: *Talanta* 71.5 (2007), pp. 2040–2047 (cited on page 52).

[271] Rajeev Jain, Nimisha Jadon, and Archana Pawaiya. 'Polypyrrole based next generation electrochemical sensors and biosensors: A review'. In: *TrAC Trends in Analytical Chemistry* 97 (2017), pp. 363–373 (cited on page 53).

[272] Gabriela Preda, Otilia Bizerea, and Beatrice Vlad-Oros. 'Sol-gel technology in enzymatic electrochemical biosensors for clinical analysis'. In: *Biosensors for Health, Environment and Biosecurity* (2011), pp. 363–368 (cited on page 53).

[273] J Griffin and M OKane. *Dip Coating: Practical Guide to Theory and Troubleshooting* (cited on page 53).

[274] Karolina Wieszczycka et al. 'Surface functionalization–The way for advanced applications of smart materials'. In: *Coordination Chemistry Reviews* 436 (2021), p. 213846 (cited on page 53).

[275] MB Kupletskaya et al. 'Search for lactate oxidase producer microorganisms'. In: *Applied Biochemistry and Microbiology* 43 (2007), pp. 178–181 (cited on page 53).

[276] Ingar Leiros et al. 'The 2.1 Å structure of Aerococcus viridans L-lactate oxidase (LOX)'. In: *Acta Crystallographica Section F: Structural Biology and Crystallization Communications* 62.12 (2006), pp. 1185–1190 (cited on page 53).

[277] Hoang Hiep Nguyen et al. 'Immobilized enzymes in biosensor applications'. In: *Materials* 12.1 (2019), p. 121 (cited on page 54).

[278] Ahmad Abolpour Homaei et al. 'Enzyme immobilization: an update'. In: *Journal of chemical biology* 6.4 (2013), pp. 185–205 (cited on page 54).

[279] Jianxin Zhang et al. 'Micro-and macrothermal analysis of a bioactive surface-engineered polymer formed by physical entrapment of poly (ethylene glycol) into poly (lactic acid)'. In: *Macromolecules* 36.4 (2003), pp. 1215–1221 (cited on page 54).

[280] *Introducing the Form 3 and Form 3L, Powered by Low Force Stereolithography - formlabs.com*. https://formlabs.com/blog/introducing-form-3-form-3l-low-force-stereolithography/. Accessed 15-09-2023 (cited on page 55).

[281] *BioMed Clear Resin - formlabs.com*. https://formlabs.com/store/materials/biomed-clear-resin/. Accessed 15-09-2023 (cited on page 55).

[282] *Guide to Post-Processing and Finishing SLA Resin 3D Prints — formlabs.com*. https://formlabs.com/blog/post-processing-and-finishing-sla-prints/. Accessed 15-09-2023 (cited on page 56).

[283] *PT1 Platinum Paste - greatcellsolarmaterials.com*. https://www.greatcellsolarmaterials.com/pt1-platinum-paste.html. Accessed 15-09-2023. Nov. 2020 (cited on page 56).

[284] *PSTrace - PalmSens - palmsens.com*. https://www.palmsens.com/software/ps-trace/. Accessed 15-09-2023. Jul. 2019 (cited on page 57).

[285] Formlabs. *Formlabs Customer Support — support.formlabs.com*. https://support.formlabs.com/s/article/What-is-the-melting-point-of-Formlabs-resins?. Accessed 15-09-2023 (cited on page 59).

[286] Nanochemazone. *Platinum Paste Screen Print Ink - Nanochemazone - nanochemazone.com*. https://www.nanochemazone.com/product/platinum-paste-screen-print-ink/. Accessed 15-09-2023 (cited on page 59).
[287] Vivien Perrelle. *Bione - cables.gl*. https://cables.gl/p/5jtYEl. Accessed 15-09-2023. 2023 (cited on page 60).
[288] *Cables - cables.gl*. https://cables.gl/home. Accessed 15-09-2023 (cited on page 60).
[289] Céline Demonsant. 'Toward intuitive interfaces for art and science'. 2022 (cited on page 60).